

**Cross Sections for the Cu(n,xn) and Cu(n,xγ) Reactions Between 1 and 20 MeV**

G. L. Morgan

**OAK RIDGE NATIONAL LABORATORY**  
**OPERATED BY UNION CARBIDE CORPORATION · FOR THE DEPARTMENT OF ENERGY**

Printed in the United States of America. Available from  
National Technical Information Service  
U.S. Department of Commerce  
5285 Port Royal Road, Springfield, Virginia 22161  
Price: Printed Copy \$4.50; Microfiche \$3.00

This report was prepared as an account of work sponsored by an agency of the United States Government. Neither the United States Government nor any agency thereof, nor any of their employees, contractors, subcontractors, or their employees, makes any warranty, express or implied, nor assumes any legal liability or responsibility for any third party's use or the results of such use of any information, apparatus, product or process disclosed in this report, nor represents that its use by such third party would not infringe privately owned rights.

ORNL-5499  
ENDF-273  
Dist. Category UC-34c

Contract No. W-7405-eng-26

Engineering Physics Division

CROSS SECTIONS FOR THE Cu( $n,xn$ ) AND Cu( $n,x\gamma$ ) REACTIONS  
BETWEEN 1 AND 20 MeV

G. L. Morgan

Date Published: February, 1979

OAK RIDGE NATIONAL LABORATORY  
Oak Ridge, Tennessee 37830  
operated by  
UNION CARBIDE CORPORATION  
for the  
DEPARTMENT OF ENERGY



## ABSTRACT

Differential cross sections for the production of secondary neutrons and gamma rays from neutron interactions in natural copper have been measured at 130 deg. (lab) for incident neutron energies in the range 1 to 20 MeV. An electron linac was used as a pulsed, white neutron source. Incident neutron energies were determined using time-of-flight techniques for a source-to-sample distance of 48 m. Secondary spectra were determined by unfolding the pulse-height distributions observed in a NE-213 scintillation counter. The results are compared to the current evaluated nuclear data file (ENDF/B-IV, MAT 1295).



## INTRODUCTION

In recent years it has become clear that copper will be a major constituent of practical fusion reactors. Most conceptual design studies (see for example Ref. 1) use the evaluated nuclear data files (e.g. ENDF/B) as the source of basic microscopic cross-section data.

The interaction of neutrons in a structural material can profoundly affect the neutron spectrum and can give rise to secondary gamma radiation. Thus the accuracy of the prediction of design criteria such as tritium breeding ratios, radiation damage, and neutron-induced heating is dependent on the accuracy of the evaluated data for energies up to the primary energy of 14 MeV.

The existing experimental data on copper cross sections have been assembled, evaluated, and supplemented with model calculations by Drake and Fricke<sup>2</sup> to form the most recent data file for this nuclide (ENDF/B-IV, MAT 1295). The purpose of the measurements reported here was to provide data to test some aspects of this evaluated cross-section file in the MeV region. The work was performed as part of a program at the Oak Ridge National Laboratory<sup>3-15</sup> to check evaluated files for those elements that are important in applied problems dealing with weapons radiation, reactor shielding, and fusion technology.

The technique used here has the global testing power of an integral experiment, yet retains a sufficiently differential character to allow localization of discrepancies. The data presented here provide some important tests of evaluated cross sections over wide ranges of incident and secondary energies. Of particular value for copper are data on the large cross sections for the production of low-energy secondary

neutrons produced by incident neutrons with energies above 8 MeV.

Measurements with the more conventional neutron sources such as Van de Graaff accelerators are difficult, if not impossible, in this region (except near 14 MeV).

Differential cross sections are presented for the Cu(n,xn) and Cu(n,x $\gamma$ ) reactions as a function of the incident neutron energy at an average scattering angle of 130 deg. (lab). The data cover the incident-neutron energy range from 1 to 20 MeV. Comparisons are presented with cross sections obtained from the evaluation.

#### EXPERIMENTAL PROCEDURE

The experimental procedure used in this work has been described in detail elsewhere<sup>16</sup> and is only briefly outlined here. The Oak Ridge Electron Linear Accelerator (ORELA) was used as a white neutron source. An electron-beam pulse width of 20 nsec at a repetition rate of 800 sec<sup>-1</sup> was employed. A beam time of 200 h was necessary for completion of the measurement.

The scattering sample was located 47.8 m from the neutron source and consisted of 1872 g of copper (> 99% purity) formed in an annular ring about 25 cm in o.d., 15 cm in i.d., and with a thickness of 0.65 cm (= 0.0548 atom/b). Secondary radiation from the sample was detected by an NE-213 scintillation counter<sup>17</sup> located on the axis of the ring at a position corresponding to an average scattering angle of 130 deg. A shadow bar shielded the detector from the direct neutron beam.

The energy of the incident neutron was determined by the time after the electron pulse at which the neutron-induced radiation from the sample

was detected. Each event in the detector was identified as either a neutron or gamma ray by pulse-shape discrimination techniques. The event was then recorded in a two-parameter array of pulse height versus time-of-flight (one each for secondary neutrons and secondary gamma rays).

Backgrounds were determined by measurement with the sample removed. For secondary gamma-rays the background was everywhere less than 10%. For secondary neutrons the background was worst at the highest incident neutron energies where it varied from 10% at the lowest pulse heights to about 50% at the highest pulse heights (corresponding to elastically scattered neutrons).

The neutron flux incident on the sample was measured with the NE-213 detector using one-parameter time-of-flight techniques. The sample and shadow bar were not in place for these measurements. A flux monitor consisting of a small plastic scintillator located in the edge of the neutron beam 30 m from the source was used to normalize the flux measurement to the actual cross-section measurement. The flux determination had an absolute uncertainty of  $\sim 10\%$  and is the largest source of systematic error in the cross sections reported here.

#### DATA REDUCTION

Two methods of data reduction were employed, each intended to make use of the available counting statistics to provide a maximum of information about a particular aspect of the cross section. In the first, the neutron or gamma-ray pulse-height spectra were integrated over intervals of neutron time-of-flight to form pulse-height spectra for specific incident neutron energy ranges. These intervals ranged in width

from  $\Delta E_{inc} = 0.25$  MeV at  $E_{inc} = 1$  MeV to  $\Delta E_{inc} = 2.5$  MeV at  $E_{inc} = 20$  MeV. The pulse-height spectra so formed were then converted to neutron or gamma-ray energy distributions by unfolding with the FERD code<sup>18</sup> using the measured neutron or gamma-ray response functions of the NE-213 detector. These distributions were then normalized to cross sections using the measured neutron flux, average sample-to-detector distance, and sample thickness.

Both neutron and gamma-ray results were corrected for finite sample effects. These corrections consisted of three terms: 1) the average transmission of the incident neutron flux, 2) the average transmission out of the sample by the secondary neutrons or gamma-rays, and 3) the fraction of events reaching the detector due to multiple interactions in the sample. The magnitudes of these corrections were calculated using a Monte Carlo method. Neutron cross sections for this calculation were generated from the evaluated data<sup>2</sup> by the AMPX code system.<sup>19</sup>

Forty neutron groups were used in this calculation covering neutron energies from 0.5 to 20 MeV. Twenty gamma-ray group cross sections were generated from the data of Ref. 20 covering gamma-ray energies from 0.3 to 10 MeV. Both neutron and gamma-ray group widths were varied so as to maintain about a 10% relative width. The gamma-ray total interaction cross sections were taken from the tables of Ref. 21.

The calculated transmissions depend only on the total cross sections and the accuracy for these terms in the correction is better than 3% since the total cross sections are accurately known. The uncertainty in the multiple scattering correction is dependent on how well the evaluated data describe the neutron interactions. To allow for any inaccuracies in

the evaluation, an uncertainty of 10% was assigned to the multiple scattering component and this error was then propagated through the succeeding analysis.

The unfolded data described above provide detailed information about the secondary neutron and gamma-ray spectra, but because the unfolding technique requires good statistical accuracy, the data must be binned over rather large incident energy intervals. Therefore, a second type of data reduction, pulse-height weighting,<sup>16,22</sup> was also used. This technique provided only integral information about the secondary spectra (i.e., total yield and average energy), but because the demands on statistical accuracy are less severe, it allowed better resolution in the incident neutron energy. For this work, the pulse-height weighting analysis was applied to spectra formed by integration over time-of-flight intervals corresponding to  $\Delta E_{inc} = 0.05$  MeV at  $E_{inc} = 1$  MeV and increasing to  $\Delta E_{inc} = 0.5$  MeV at  $E_{inc} = 20$  MeV. The finite sample effects described above were also applied to these data. The final results of this analysis are total yield of secondary neutrons and secondary gamma rays and their average energies as a function of incident neutron energy.

#### DISCUSSION

The work reported here provides data to test the evaluated secondary cross sections over a wide range of energies. The experimental resolution in the incident energy ( $\sim 0.4$  nsec/m contributed by electron pulse width and sample-to-detector time lag) is very good, so resolution in the final data is limited only by the bin widths necessary for adequate statistical accuracy. Energy resolution for the secondary spectra is due to the NE-213

detector's pulse-height resolution and is rather poor. This resolution does not permit unique identification of the various reactions contributing to the secondary spectra. Because of this inability to completely resolve the different contributions to the secondary spectra, results have been obtained only as laboratory-system cross sections. These data are shown in Figs. 1-14. The uncertainties shown do not include an estimated 10% uncertainty in overall normalization.

The incident neutron energy spread, the secondary energy resolution, and the angular spread are much broader in this measurement than in the more standard types of differential cross-section measurements. This has the advantage of allowing a comprehensive check of the cross sections in a mode that is compatible with the averaging generally used to produce group cross sections for practical applications. However, it complicates and sometimes makes impossible the comparison of the present results with previous measurements. To correctly average over the experimental spreads, one needs a complete prescription for cross sections as a function of incident energy, scattering angle, Q-value, etc. The evaluated file provides this information and reflects previous measurements to the extent that the evaluators base their results on existing data.

Secondary neutron and gamma-ray spectra were generated from the evaluation<sup>2</sup> by suitably weighted averages over the incident energy interval and angular spread. This was accomplished using group cross sections generated with the AMPX code system. The group structure was chosen to provide about 3 groups per resolution width with a  $P_{12}$  expansion of the neutron cross sections and a  $P_0$  expansion for the gamma-ray production cross sections. The resulting secondary spectra were then smeared by

a Gaussian function corresponding to the resolution of the detector. For neutrons, the Gaussian had a resolution width defined as

$$R = \sqrt{300 + 800/E_n}$$

where  $R$  = fractional FWHM in percent and  $E_n$  is neutron energy in MeV. For gamma rays the corresponding resolution was

$$R = \sqrt{170 + 288/E_\gamma} .$$

Curves for comparison to the pulse-height weighting results were produced by integration of secondary neutron or gamma-ray spectra calculated as described above for the smaller incident energy intervals used in the pulse-height weighting analysis.

Several cautions are in order in regard to any comparison of evaluation and measurement. The gamma-ray emission specified in the evaluation is isotropic. For a medium-weight nuclide such as copper this is undoubtedly very close to the real angular dependence. Thus a comparison of the evaluation with differential measurements taken at 130 deg. checks the gamma-ray production data of the evaluation rather well. In the case of the neutron emission spectra, the test may not be as rigorous, especially with respect to the elastic scattering cross sections. Because of the strong anisotropy of the elastic angular distribution with its energy dependent diffraction pattern, a single differential measurement covering a large angular range (the angular resolution function is approximately triangular with a base 28 deg. in width) provides little or no check on the validity of the elastic scattering cross section in the evaluation. However, for neutron emission through processes other than

elastic scattering, the situation is much better since most such emissions are only weakly anisotropic, particularly when averaged over the broad incident neutron energies of this experiment.

#### SUMMARY

Measurements have been made of the secondary neutron and gamma-ray production cross sections for natural copper. The data were taken at 130 deg. and cover incident neutron energies from 1 to 20 MeV. Comparisons between the measurement and evaluation are shown in Figs. 1-14. Numerical values of the measured cross sections are given in Tables 1-3.

#### ACKNOWLEDGEMENTS

The author wishes to thank J. W. McConnell and J. G. Craven for their assistance with electronics and data acquisition computers and H. A. Todd and the ORELA staff for operation of the accelerator. Special thanks are due W. E. Ford for his help with generation of the multigroup cross sections using AMPX.

## REFERENCES

1. D. E. Bartine, R. G. Alsmiller, Jr., E. M. Oblow, and F. R. Mynatt, Nucl. Sci. Eng. 53, 304 (1974).
2. M. K. Drake and M. P. Fricke, Copper Evaluation, ENDF/B-IV MAT 1295, SAI Report DNA 3356F (1974).
3. G. L. Morgan, T. A. Love, and F. G. Perey, "Integral Neutron Scattering Measurements on Carbon from 1 to 20 MeV," ORNL-TM-4157, Oak Ridge National Laboratory (1973).
4. G. L. Morgan, T. A. Love, and F. G. Perey, "Integral Neutron Scattering Measurements on Iron from 1 to 20 MeV," ORNL-TM-4193, Oak Ridge National Laboratory (1973).
5. G. L. Morgan, "Measurement of Secondary Neutrons and Gamma Rays Produced by Neutron Bombardment of Water over the Incident Energy Range 1 to 20 MeV," ORNL-TM-5018, Oak Ridge National Laboratory (1975).
6. G. L. Morgan, "Measurement of Secondary Neutrons and Gamma Rays Produced by Neutron Interactions with Nitrogen and Oxygen over the Incident Energy Range 1 to 20 MeV," ORNL-TM-5023, Oak Ridge National Laboratory (1975).
7. S. N. Cramer and E. M. Oblow, Nucl. Sci. Eng. 58, 33 (1975).
8. G. L. Morgan, "Measurement of Secondary Neutrons and Gamma Rays Produced by Neutron Interactions in Silicon Dioxide over the Incident Energy Range 1 to 20 MeV," ORNL-TM-5024, Oak Ridge National Laboratory (1975).
9. G. L. Morgan and F. G. Perey, Nucl. Sci. Eng. 61, 337 (1976).
10. S. N. Cramer and E. M. Oblow, "Analysis of Neutron Scattering and Gamma-Ray Production Integral Experiments on Nitrogen for Neutron Energies from 1 to 15 MeV," ORNL-TM-5220, Oak Ridge National Laboratory (1976).
11. S. N. Cramer and E. M. Oblow, "Analysis of a Neutron Scattering and Gamma-Ray Production Integral Experiment on Oxygen for Neutron Energies from 1 to 15 MeV," ORNL-TM-5535, Oak Ridge National Laboratory (1976).
12. S. N. Cramer and E. M. Oblow, "Analysis of a Neutron Scattering Integral Experiment on Iron for Neutron Energies from 1 to 15 MeV," ORNL/TM-5548, Oak Ridge National Laboratory (1977).
13. G. L. Morgan, "Secondary Neutron Spectra from Neutron Interactions in a Thick Carbon Sample," ORNL/TM-5814, Oak Ridge National Laboratory (1977).

14. G. L. Morgan and F. G. Perey, "Cross Sections for the Nb(n,xn) and Nb(n,x $\gamma$ ) Reactions Between 1 and 20 MeV," ORNL/TM-5829, Oak Ridge National Laboratory (1977).
15. G. L. Morgan, "Cross Sections for the  $^7\text{Li}(n,xn)$  and  $^7\text{Li}(n,n'\gamma)$  Reactions Between 0.5 and 20 MeV," ORNL/TM-6247, Oak Ridge National Laboratory (1978).
16. G. L. Morgan, T. A. Love, and F. G. Perey, Nucl. Instrum. Methods 128, 125 (1975).
17. The NE-213 scintillation counters are available from Nuclear Enterprises, Palo Alto, California.
18. W. R. Burrus and V. V. Verbinski, Nucl. Instrum. Methods 67, 181 (1969).
19. N. M. Greene et al., "AMPX-A Modular Code System to Generate Coupled Multigroup Neutron-Gamma Cross Sections from ENDF/B," ORNL-TM-3706, Oak Ridge National Laboratory (1974).
20. G. T. Chapman, "The Cu(n,x $\gamma$ ) Reaction Cross Section for Incident Neutron Energies Between 0.2 and 20.0 MeV," ORNL/TM-5299 (April 1976).
21. E. Storm and H. I. Israel, Nuclear Data Tables A7, 565 (1970).
22. Frances Pleasonton, Robert L. Ferguson, and H. W. Schmitt, Phys. Rev. C 6, 1023 (1972).

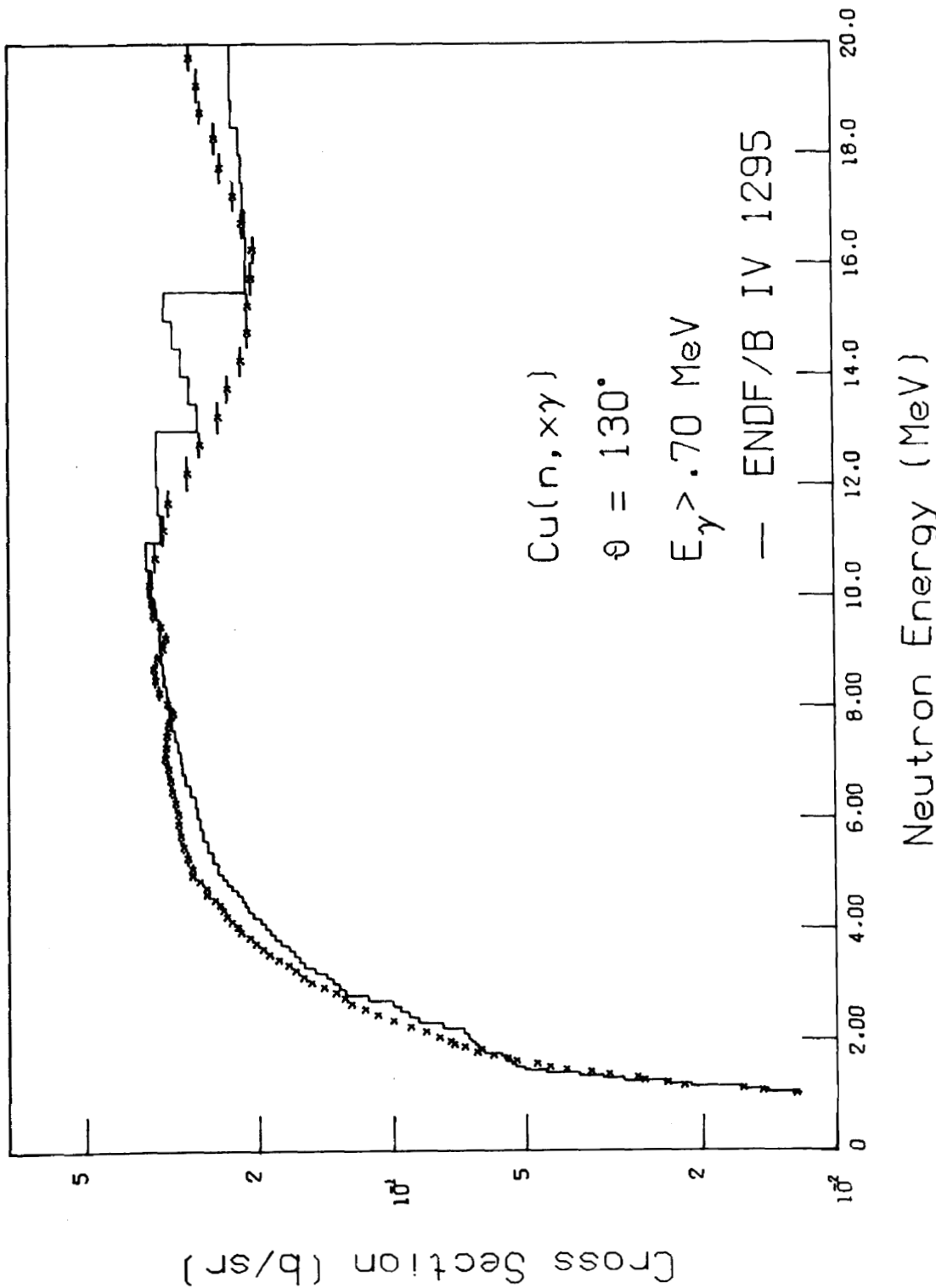


Fig. 1. Integrated yield of secondary gamma rays with  $E_\gamma > 0.7 \text{ MeV}$  as a function of the incident neutron energy.

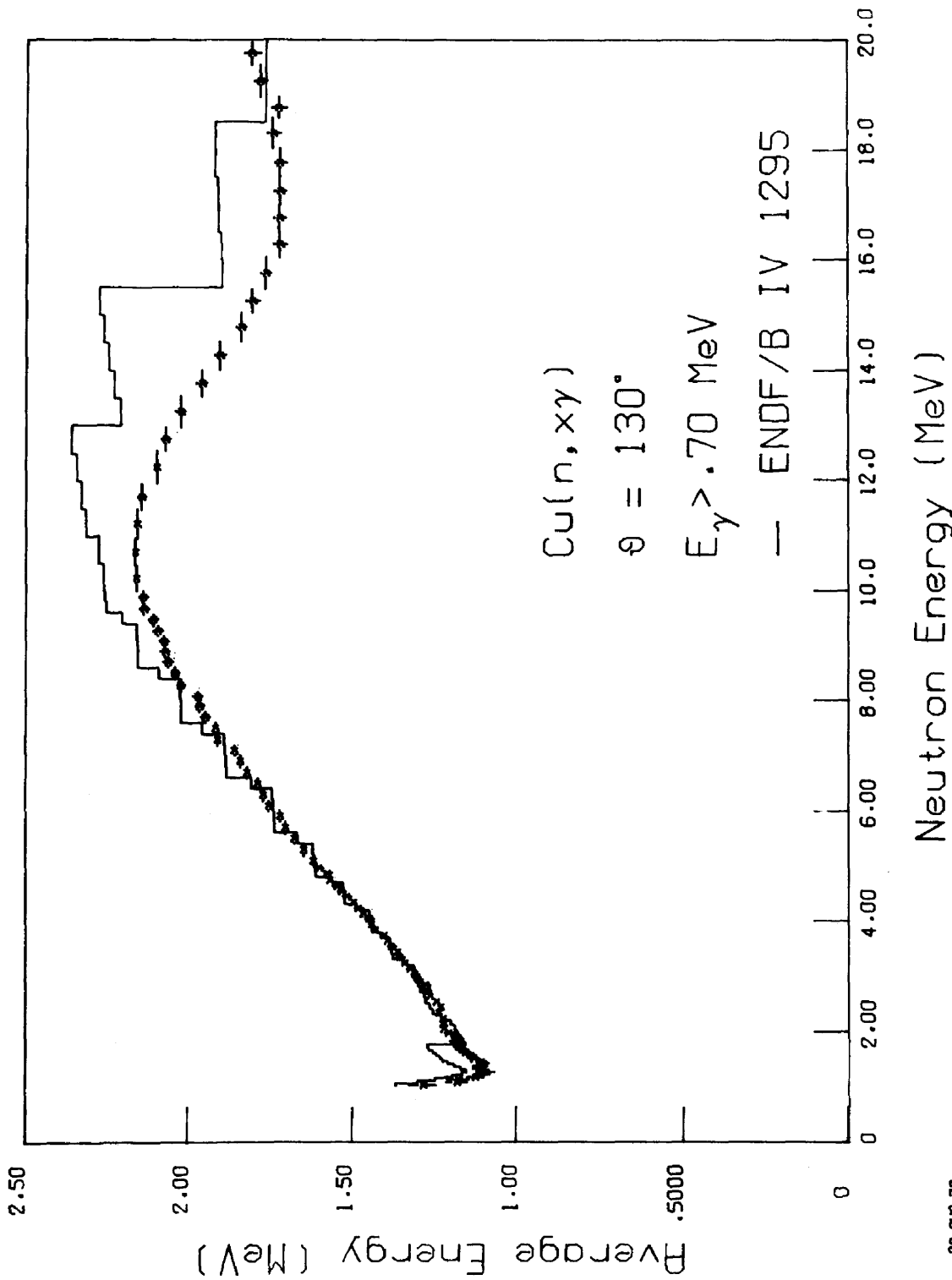


Fig. 2. Average energy of secondary gamma rays with  $E_\gamma > 0.7 \text{ MeV}$  as a function of the incident neutron energy.

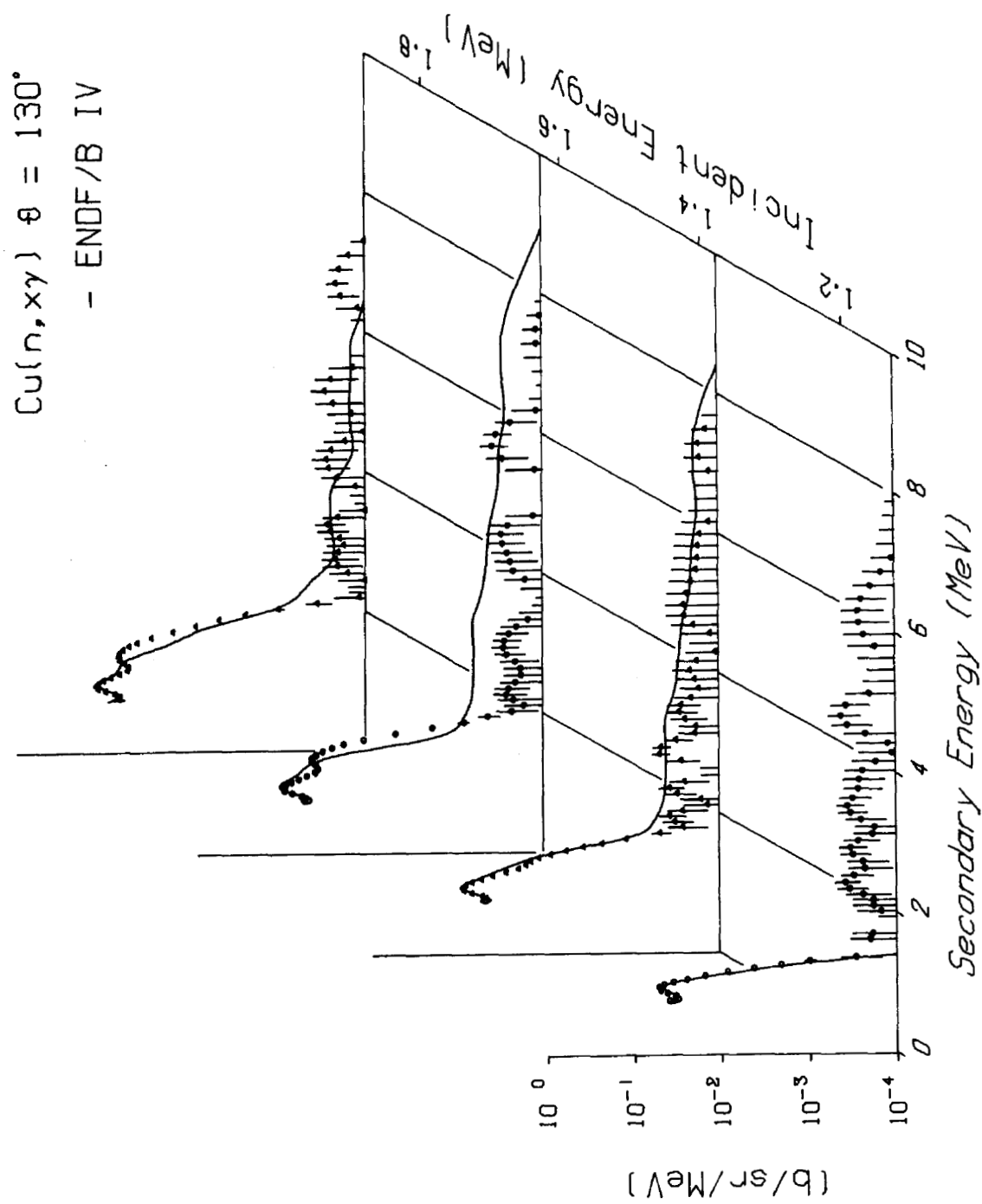


Fig. 3. Secondary gamma-ray spectra versus gamma ray and incident neutron energy.

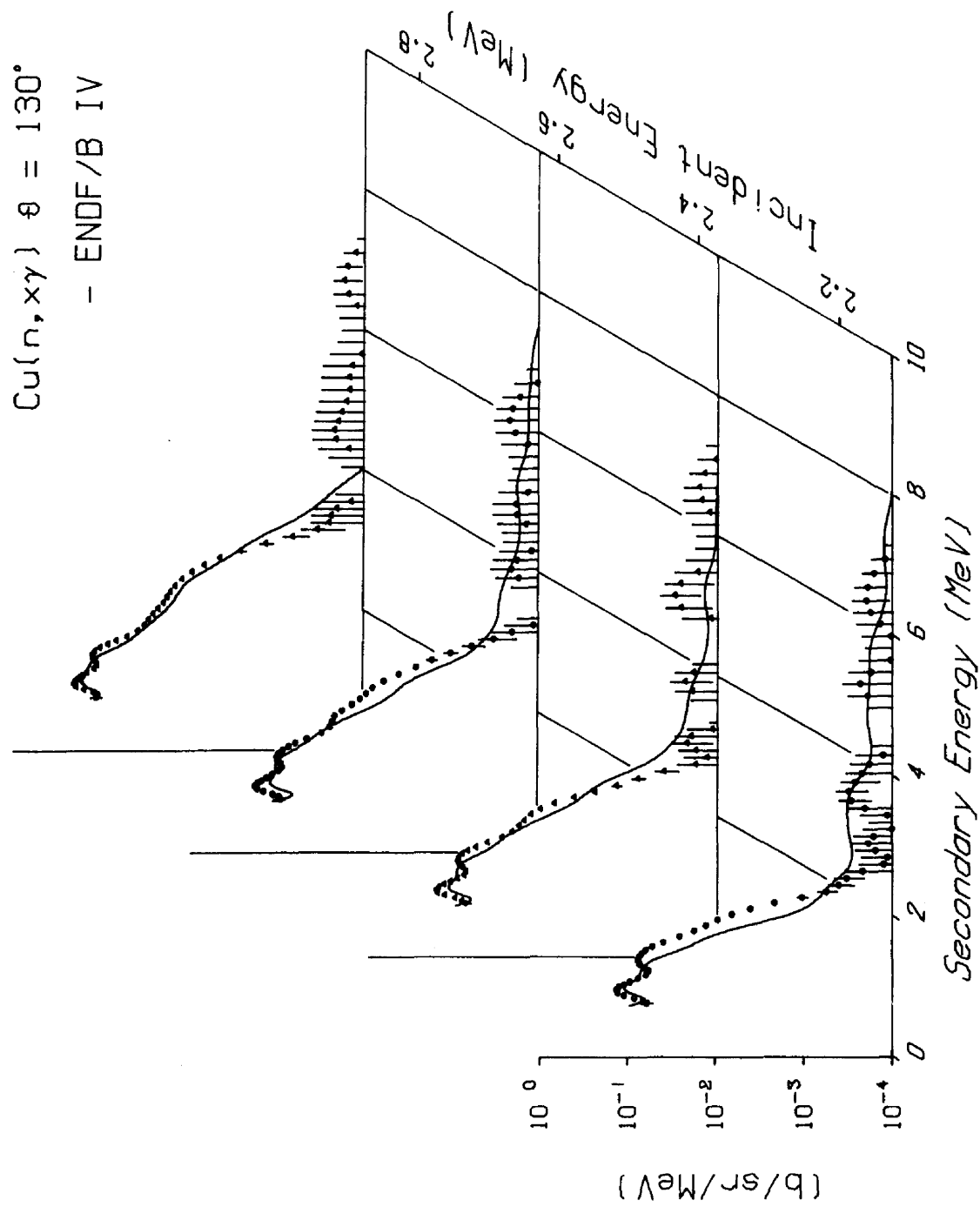


Fig. 4. Secondary gamma-ray spectra versus gamma ray and incident neutron energy.

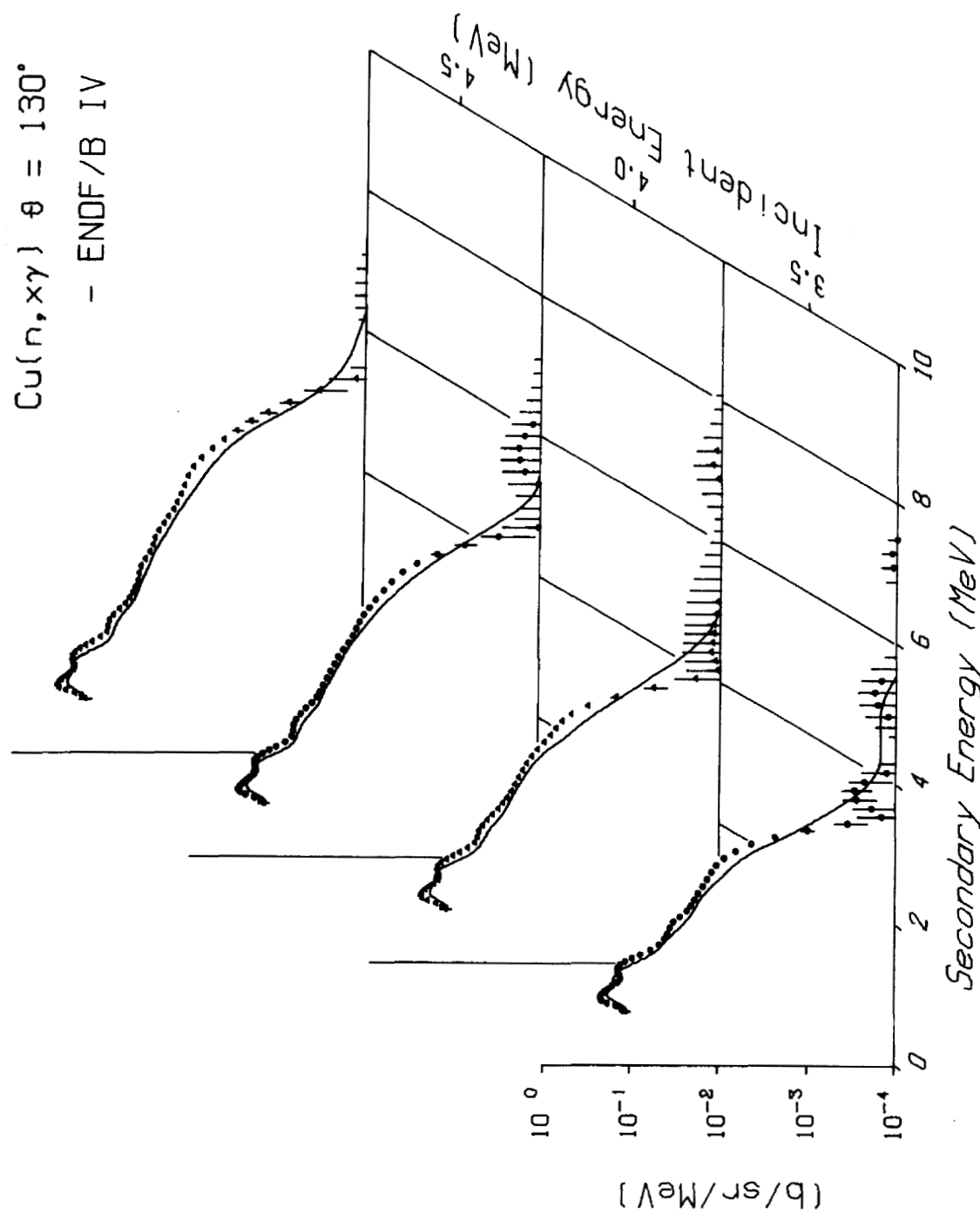


Fig. 5. Secondary gamma-ray spectra versus gamma ray and incident neutron energy.

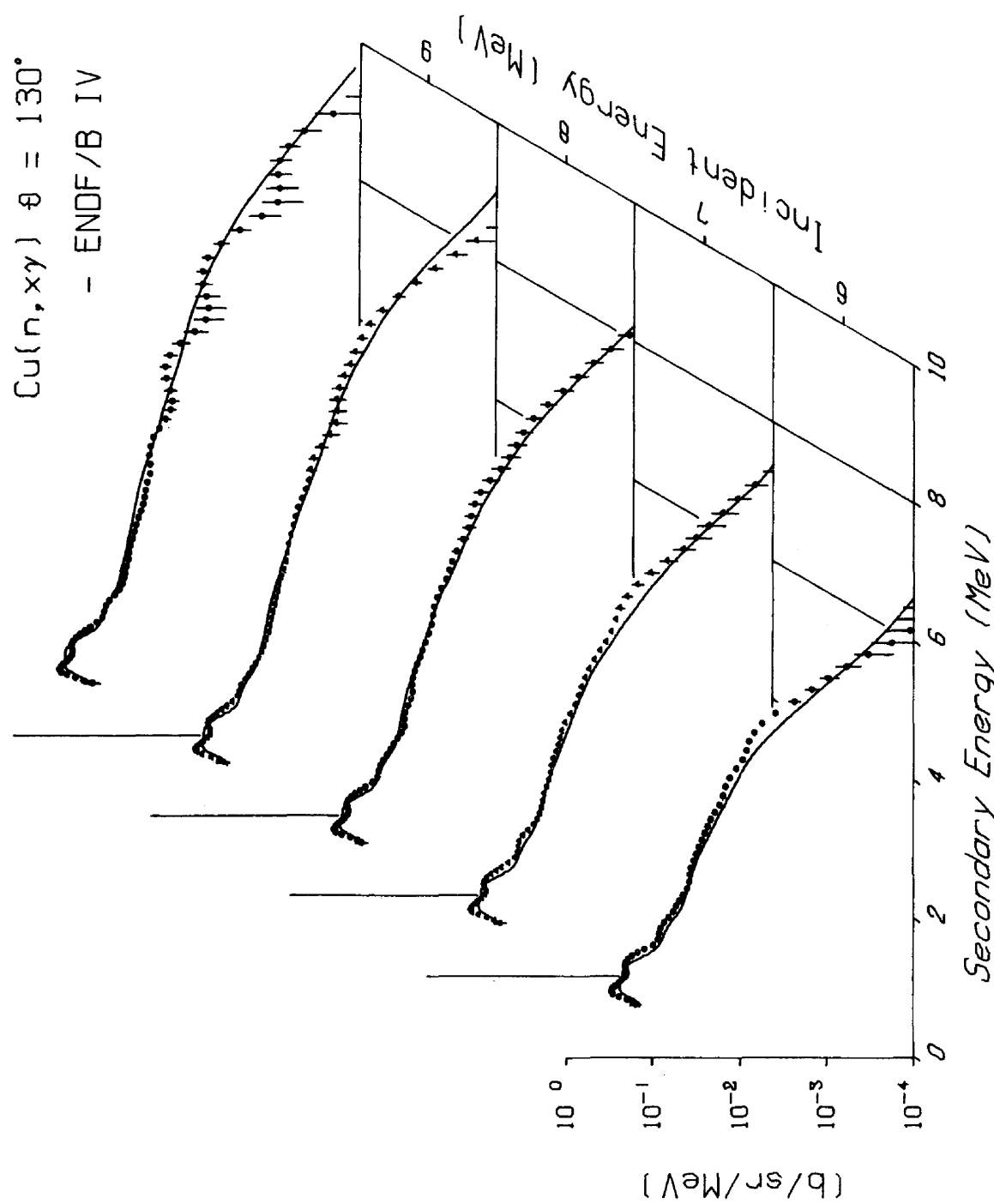


Fig. 6. Secondary gamma-ray spectra versus gamma ray and incident neutron energy.

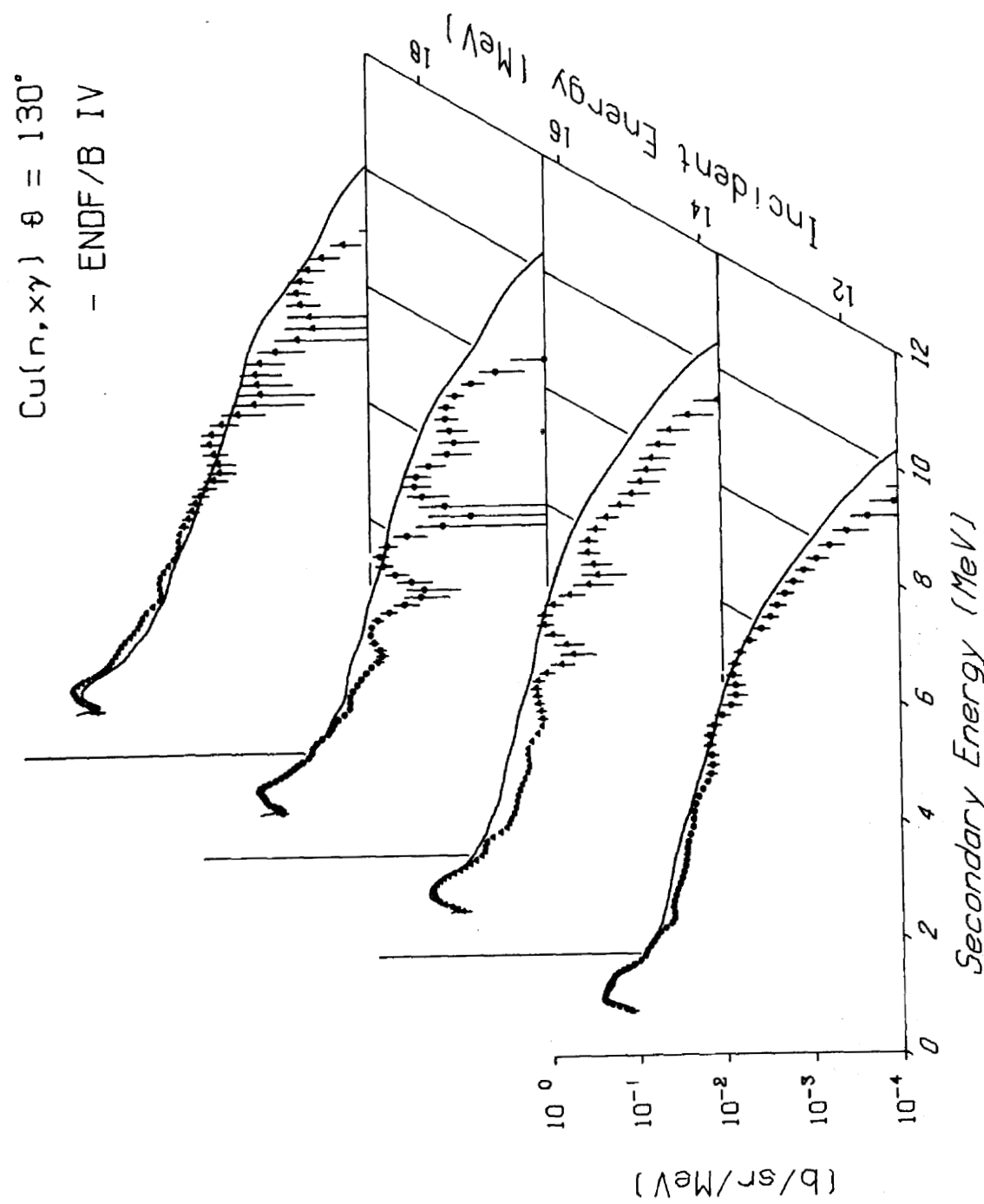


Fig. 7. Secondary gamma-ray spectra versus gamma ray and incident neutron energy.

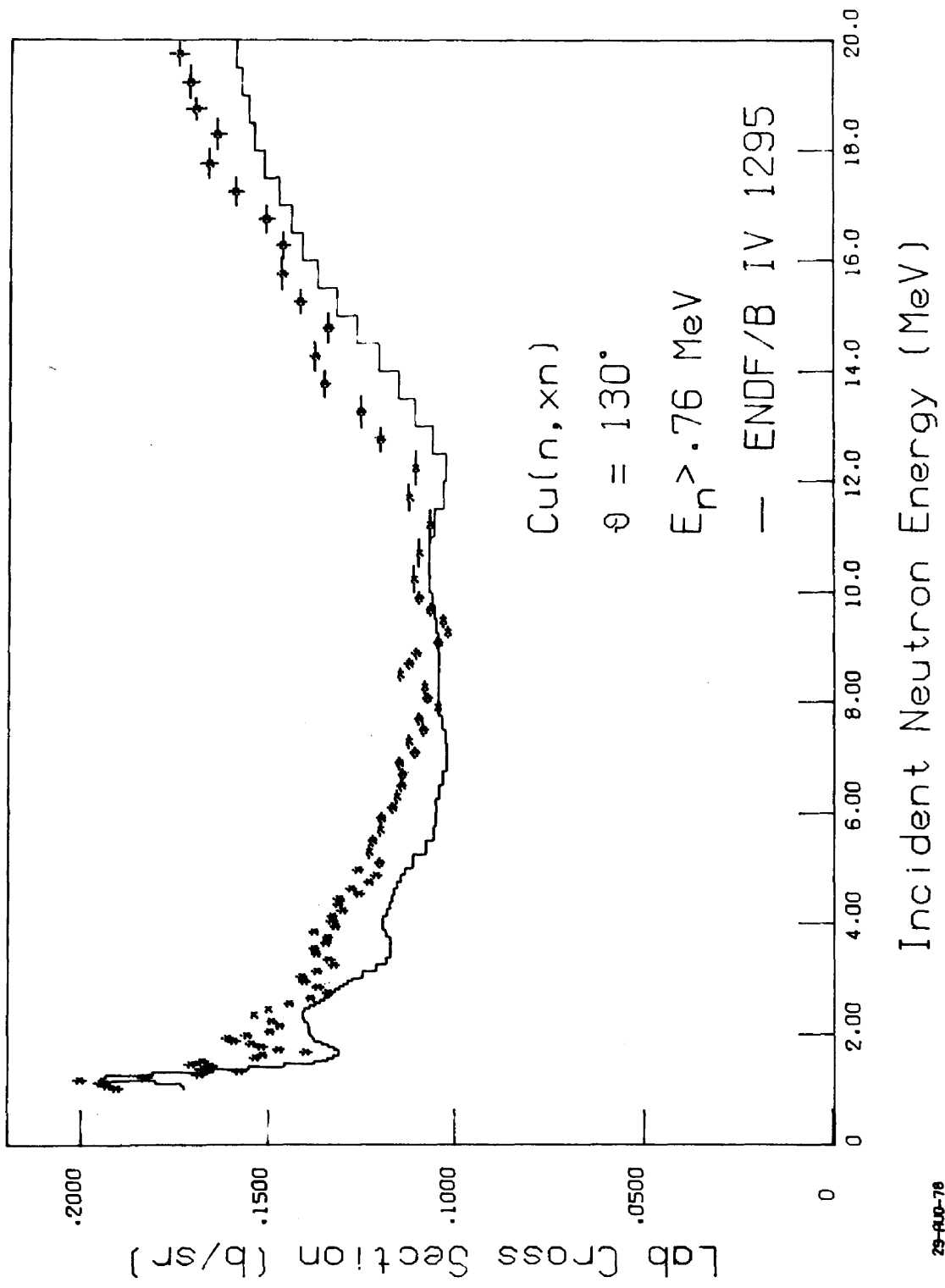


Fig. 8. Integrated yield of secondary neutrons with  $E'_n > 0.76 \text{ MeV}$  as a function of the incident neutron energy.

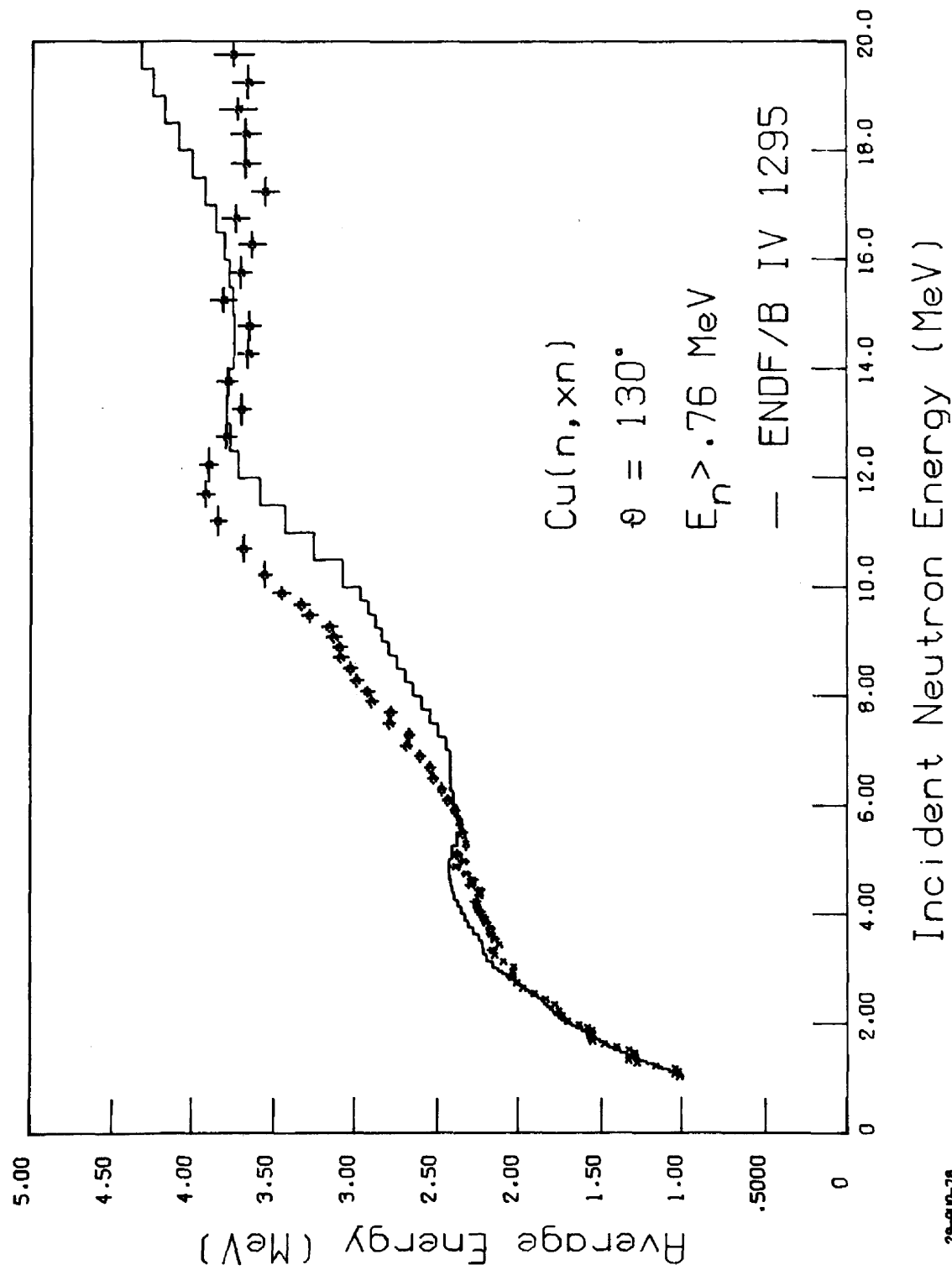


Fig. 9. Average energy of secondary neutrons with  $E'_n > 0.76$  MeV as a function of the incident neutron energy.

29-100-76

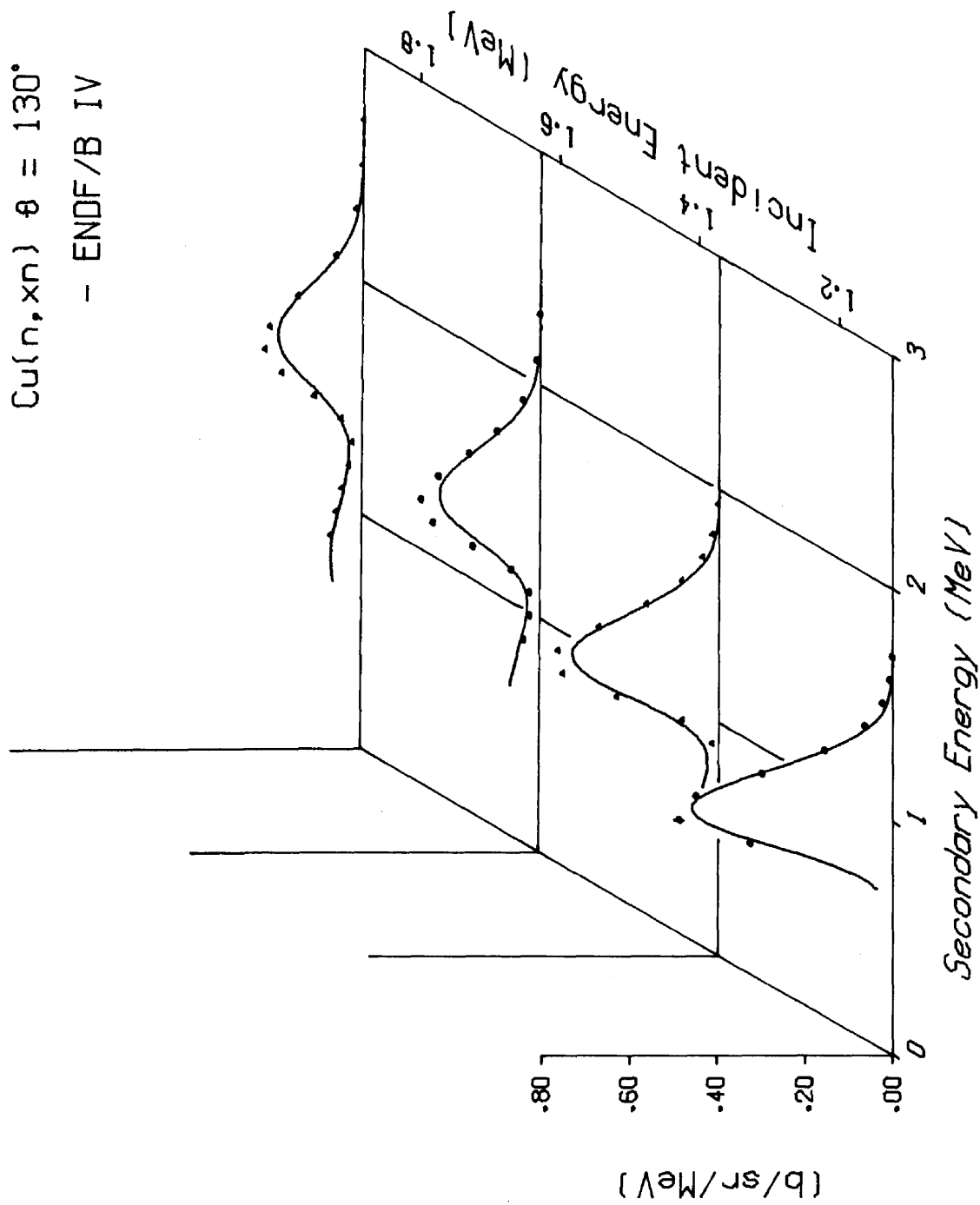


Fig. 10. Secondary neutron spectra versus scattered and incident neutron energy.

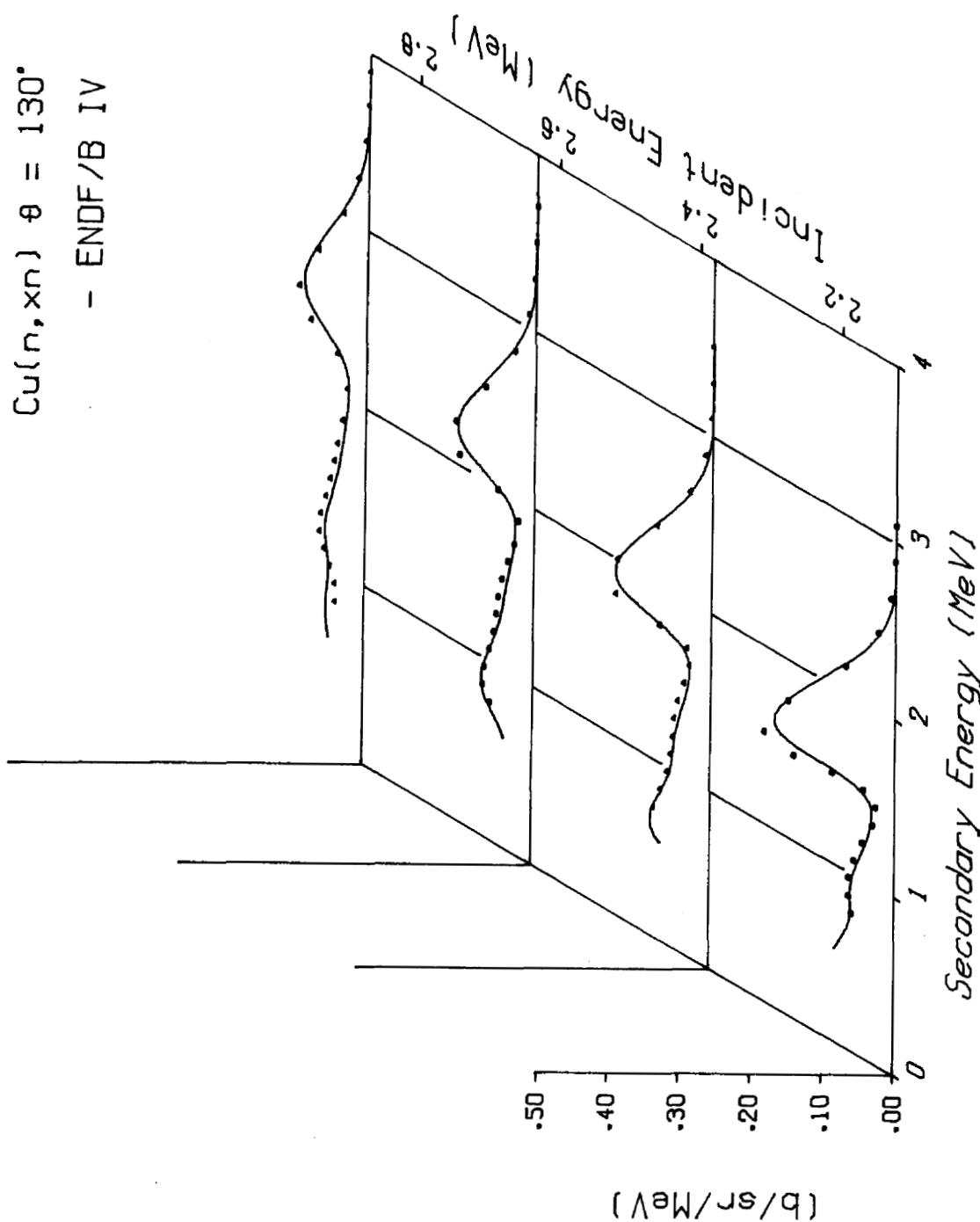


Fig. 11. Secondary neutron spectra versus scattered and incident neutron energy.

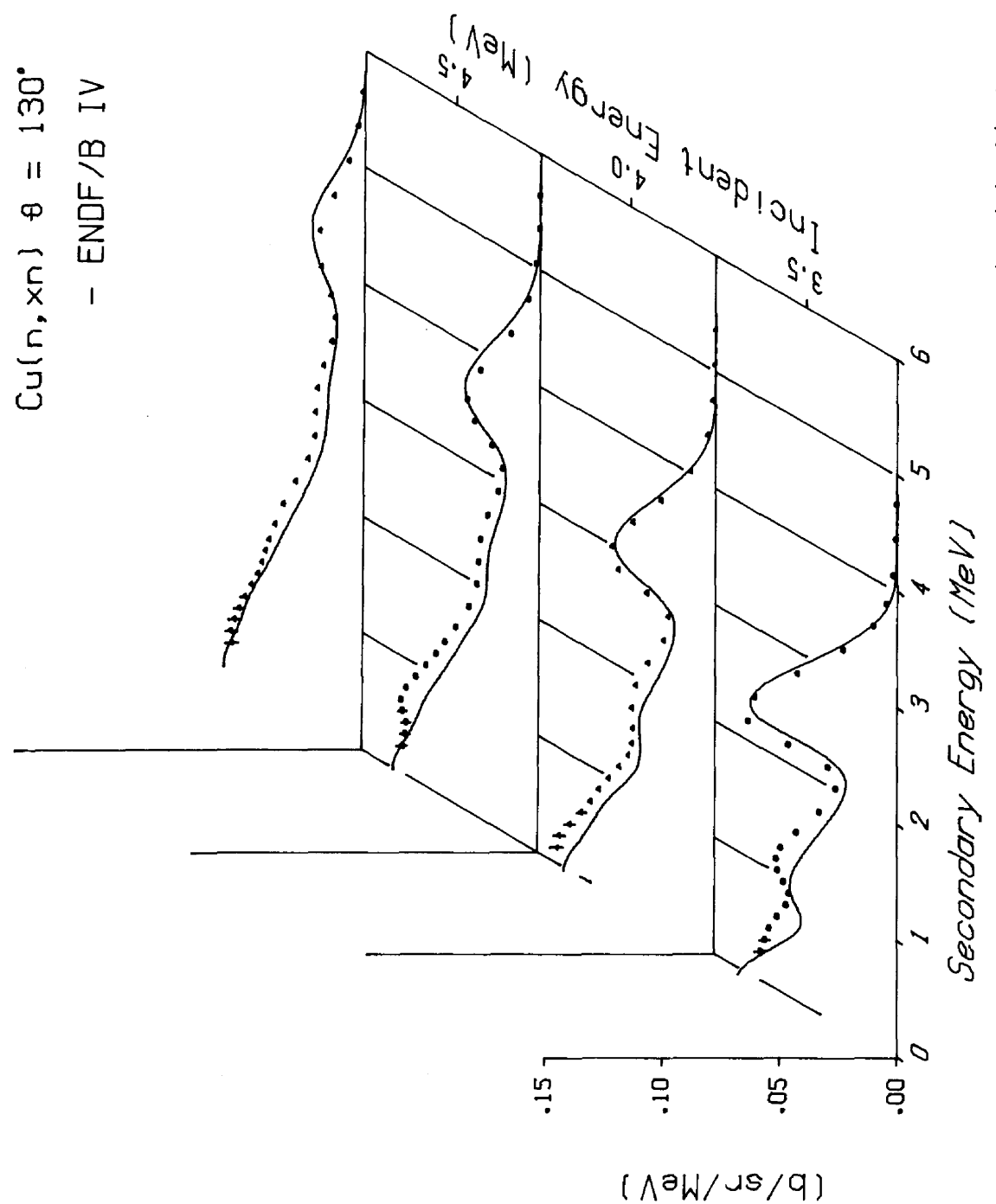


Fig. 12. Secondary neutron spectra versus scattered and incident neutron energy.

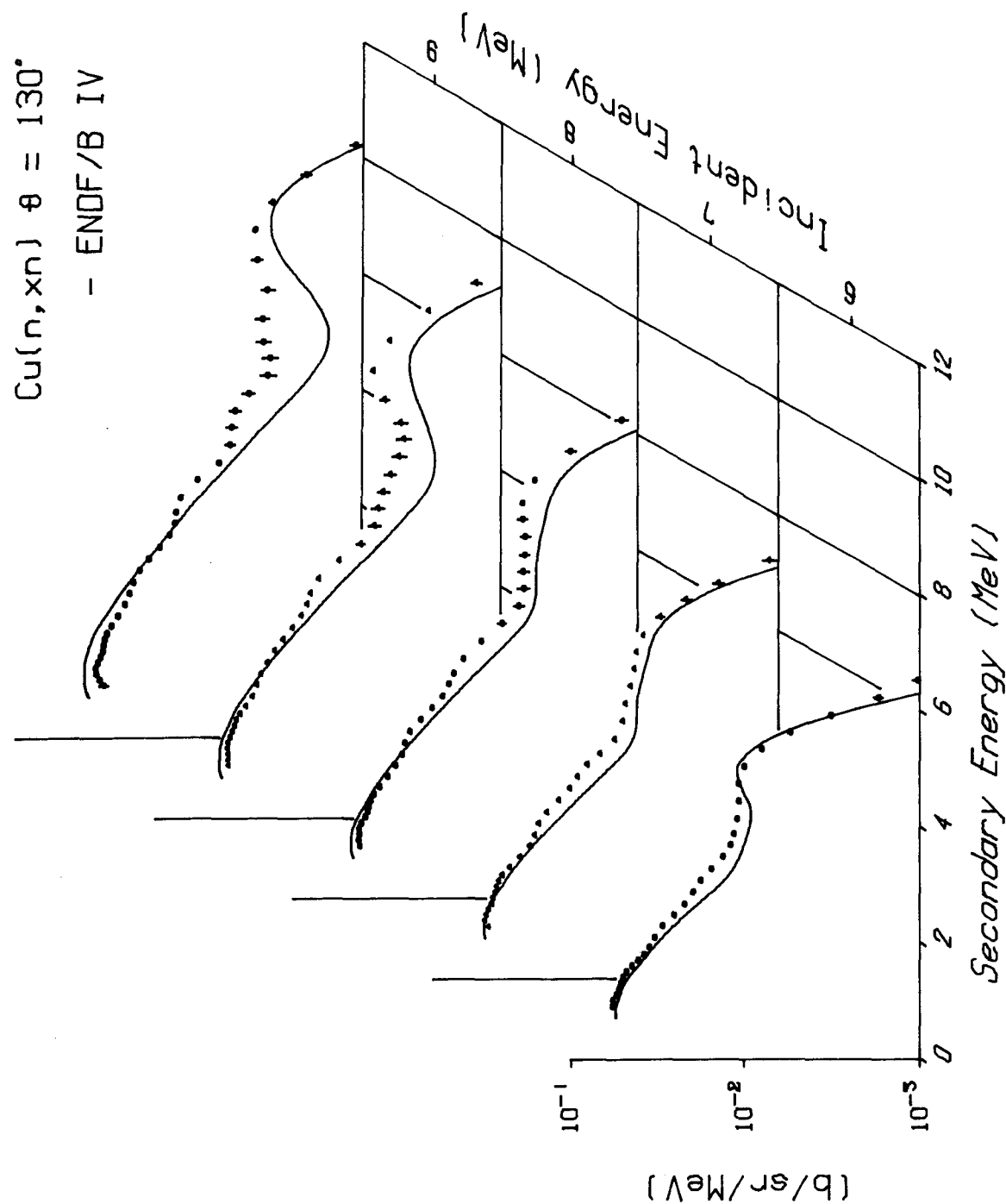


Fig. 13. Secondary neutron spectra versus scattered and incident neutron energy.

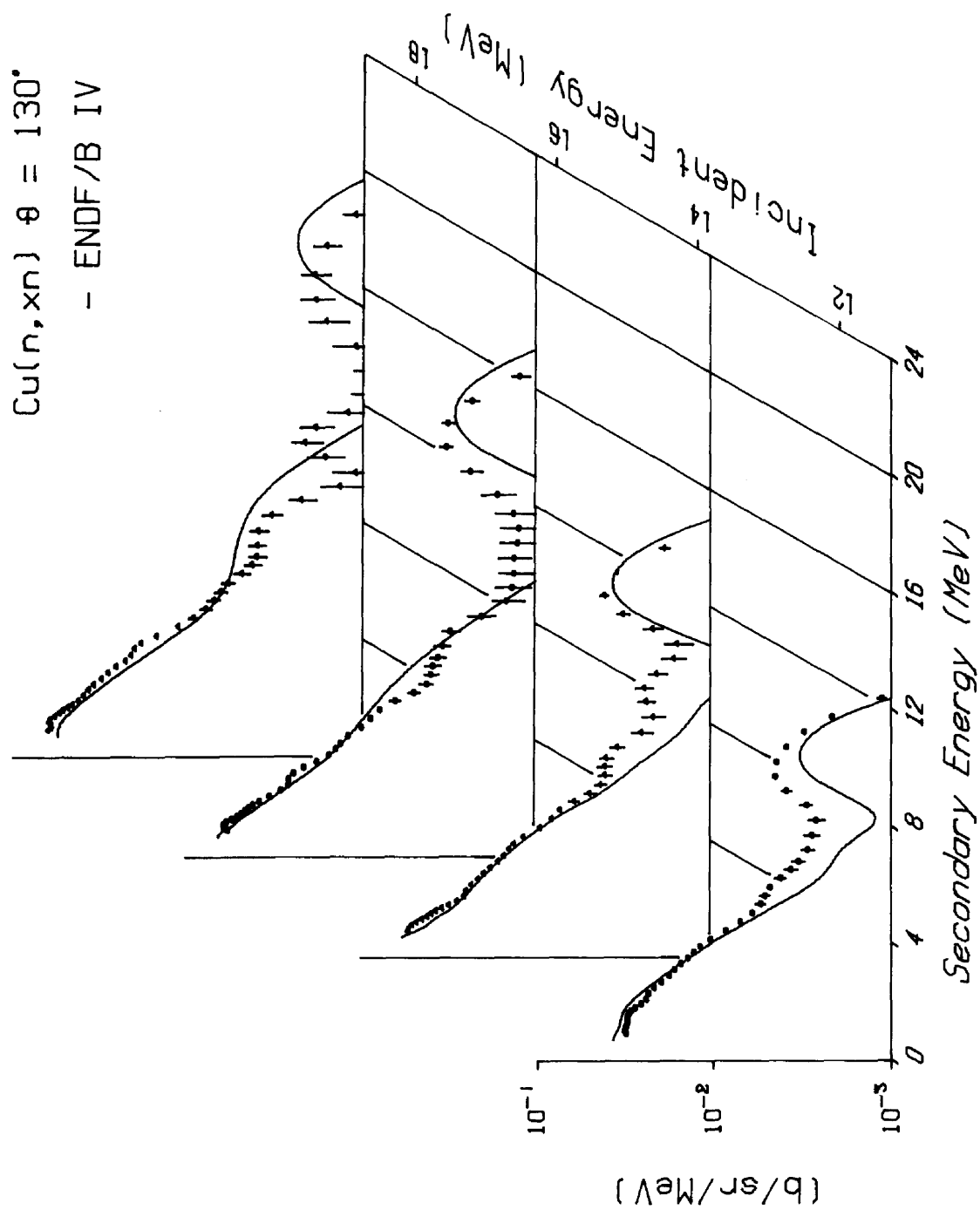


Fig. 14. Secondary neutron spectra versus scattered and incident neutron energy.

TABLE 1. CD( $n, \gamma n$ ) LABORATORY CROSS SECTIONS AT 130 DEGREES. THE NUMBERS IN PARENTHESIS ARE STATISTICAL UNCERTAINTIES (IN THE SAME UNITS AS THE DATA). THE OVERALL UNCERTAINTY IN NORMALIZATION IS ABOUT 10%.

INCIDENT ENERGY	17.50-19.96	15.05-17.50	12.55-15.05	10.01-12.55	8.99-10.01	8.01- 8.99	7.01- 8.01
SECONDARY ENERGY (MEV)	CROSS SECTION (MB/SR/MEV)						
0.909	62.0 ( 3.0)	57.0 ( 2.5)	52.9 ( 2.3)	31.3 ( 1.8)	30.6 ( 1.9)	37.1 ( 2.1)	40.8 ( 2.1)
1.013	59.5 ( 2.5)	59.0 ( 2.3)	51.7 ( 2.0)	31.8 ( 1.7)	32.0 ( 1.7)	37.6 ( 1.8)	41.5 ( 1.9)
1.114	59.1 ( 2.6)	58.0 ( 2.3)	49.9 ( 2.0)	31.5 ( 1.6)	33.9 ( 1.6)	37.5 ( 1.6)	41.2 ( 1.8)
1.212	60.9 ( 2.4)	57.7 ( 2.0)	47.0 ( 1.8)	31.2 ( 1.5)	34.2 ( 1.5)	37.8 ( 1.5)	41.3 ( 1.7)
1.310	59.9 ( 2.2)	54.0 ( 1.8)	43.6 ( 1.5)	30.9 ( 1.3)	33.2 ( 1.4)	37.6 ( 1.4)	40.2 ( 1.5)
1.413	56.4 ( 2.1)	50.3 ( 1.7)	40.8 ( 1.5)	30.9 ( 1.3)	31.8 ( 1.3)	36.4 ( 1.3)	38.2 ( 1.4)
1.511	53.2 ( 2.0)	47.5 ( 1.7)	38.8 ( 1.4)	30.9 ( 1.2)	31.0 ( 1.2)	35.2 ( 1.3)	37.0 ( 1.4)
1.611	50.7 ( 1.9)	45.4 ( 1.6)	36.5 ( 1.3)	30.4 ( 1.1)	30.6 ( 1.2)	34.3 ( 1.2)	36.4 ( 1.3)
1.709	47.7 ( 1.8)	43.2 ( 1.5)	33.8 ( 1.2)	29.4 ( 1.0)	30.2 ( 1.1)	33.3 ( 1.2)	35.7 ( 1.3)
1.807	44.7 ( 2.1)	41.0 ( 1.6)	30.8 ( 1.2)	27.9 ( 1.0)	29.4 ( 1.2)	32.0 ( 1.3)	34.3 ( 1.3)
1.938	41.8 ( 2.0)	37.7 ( 1.5)	27.6 ( 1.2)	25.8 ( 1.0)	27.8 ( 1.2)	29.7 ( 1.2)	31.8 ( 1.2)
2.112	38.6 ( 1.5)	33.2 ( 1.1)	25.1 ( 0.9)	24.2 ( 0.8)	25.6 ( 0.9)	27.2 ( 0.9)	28.6 ( 0.9)
2.310	34.6 ( 1.7)	28.4 ( 1.2)	24.3 ( 1.0)	23.4 ( 0.8)	23.3 ( 1.0)	25.8 ( 1.0)	25.5 ( 1.0)
2.499	33.9 ( 1.3)	26.0 ( 1.0)	22.8 ( 0.8)	21.7 ( 0.7)	21.8 ( 0.8)	24.4 ( 0.8)	23.6 ( 0.8)
2.693	30.9 ( 1.2)	25.5 ( 0.9)	21.0 ( 0.7)	19.7 ( 0.6)	20.6 ( 0.7)	22.5 ( 0.7)	22.8 ( 0.7)
2.898	29.2 ( 1.3)	24.0 ( 0.9)	19.4 ( 0.7)	17.9 ( 0.6)	19.0 ( 0.7)	20.2 ( 0.7)	21.2 ( 0.7)
3.102	25.2 ( 1.3)	21.0 ( 1.0)	17.8 ( 0.8)	16.6 ( 0.7)	17.0 ( 0.8)	18.1 ( 0.8)	18.4 ( 0.8)
3.301	22.3 ( 1.1)	17.9 ( 0.8)	16.1 ( 0.6)	15.3 ( 0.6)	14.8 ( 0.7)	16.1 ( 0.7)	15.7 ( 0.6)
3.505	20.7 ( 1.1)	15.3 ( 0.8)	14.9 ( 0.7)	14.0 ( 0.6)	13.0 ( 0.7)	14.3 ( 0.7)	13.8 ( 0.6)
3.712	19.7 ( 1.1)	13.9 ( 0.8)	14.0 ( 0.7)	12.9 ( 0.6)	12.1 ( 0.7)	13.3 ( 0.7)	12.7 ( 0.7)
3.901	18.1 ( 0.9)	13.1 ( 0.7)	13.1 ( 0.6)	11.9 ( 0.5)	11.9 ( 0.6)	12.7 ( 0.6)	11.9 ( 0.6)
4.147	14.9 ( 0.9)	11.9 ( 0.6)	11.5 ( 0.5)	10.4 ( 0.5)	11.2 ( 0.6)	11.3 ( 0.6)	10.5 ( 0.5)
4.457	11.2 ( 0.6)	9.9 ( 0.5)	9.3 ( 0.4)	8.5 ( 0.3)	8.9 ( 0.4)	8.7 ( 0.4)	8.2 ( 0.4)
4.754	9.1 ( 0.6)	8.8 ( 0.5)	7.9 ( 0.4)	7.1 ( 0.3)	6.8 ( 0.4)	6.5 ( 0.4)	6.2 ( 0.4)
5.057	7.8 ( 0.6)	7.8 ( 0.5)	7.1 ( 0.4)	6.0 ( 0.3)	5.8 ( 0.4)	5.5 ( 0.4)	5.0 ( 0.4)
5.360	7.0 ( 0.6)	6.4 ( 0.5)	6.0 ( 0.4)	5.5 ( 0.4)	5.8 ( 0.5)	5.2 ( 0.5)	4.7 ( 0.4)
5.644	6.5 ( 0.6)	5.0 ( 0.4)	4.9 ( 0.4)	5.2 ( 0.3)	5.5 ( 0.4)	4.9 ( 0.4)	4.7 ( 0.4)
5.936	5.8 ( 0.5)	4.2 ( 0.4)	4.2 ( 0.4)	4.8 ( 0.3)	4.6 ( 0.4)	4.5 ( 0.4)	4.6 ( 0.3)
6.251	4.9 ( 0.5)	4.0 ( 0.4)	4.0 ( 0.4)	4.2 ( 0.3)	3.6 ( 0.4)	4.0 ( 0.4)	4.6 ( 0.3)
6.551	6.3 ( 0.5)	3.9 ( 0.4)	4.0 ( 0.4)	3.7 ( 0.3)	3.5 ( 0.4)	3.7 ( 0.4)	4.7 ( 0.3)
6.833	6.0 ( 0.5)	3.6 ( 0.4)	3.9 ( 0.4)	3.1 ( 0.3)	3.8 ( 0.4)	3.9 ( 0.4)	4.7 ( 0.3)
7.227	8.0 ( 0.5)	3.4 ( 0.4)	3.4 ( 0.3)	3.0 ( 0.3)	3.8 ( 0.4)	4.8 ( 0.3)	4.0 ( 0.2)
7.726	6.0 ( 0.5)	3.1 ( 0.4)	2.5 ( 0.4)	2.8 ( 0.3)	3.6 ( 0.4)	5.6 ( 0.3)	2.5 ( 0.2)
8.252	3.3 ( 0.5)	2.1 ( 0.4)	2.1 ( 0.3)	2.7 ( 0.3)	4.1 ( 0.3)	4.5 ( 0.2)	1.3 ( 0.1)
8.770	2.2 ( 0.4)	1.5 ( 0.3)	2.4 ( 0.3)	3.0 ( 0.2)	4.2 ( 0.2)	2.7 ( 0.2)	0.7 ( 0.1)
9.242	1.8 ( 0.4)	1.0 ( 0.3)	2.4 ( 0.3)	3.9 ( 0.2)	3.4 ( 0.2)	1.8 ( 0.1)	0.4 ( 0.1)
9.719	1.1 ( 0.4)	1.3 ( 0.3)	2.0 ( 0.3)	4.5 ( 0.2)	2.1 ( 0.2)	0.7 ( 0.1)	
10.233	1.7 ( 0.4)	1.3 ( 0.3)	1.6 ( 0.3)	4.5 ( 0.2)	1.1 ( 0.1)	0.4 ( 0.1)	
10.747	2.1 ( 0.4)	1.3 ( 0.4)	1.6 ( 0.3)	3.9 ( 0.2)	0.6 ( 0.1)	0.3 ( 0.1)	
11.254	1.9 ( 0.4)	1.3 ( 0.4)	2.2 ( 0.3)	3.1 ( 0.1)			
11.759	1.3 ( 0.4)	1.0 ( 0.3)	2.2 ( 0.3)	2.2 ( 0.1)			
12.803	0.8 ( 0.8)	1.7 ( 0.4)	4.0 ( 0.3)	1.1 ( 0.1)			
13.204	0.7 ( 0.4)	2.4 ( 0.4)	3.4 ( 0.2)				
14.027	1.1 ( 0.4)	3.3 ( 0.3)	1.9 ( 0.1)				
14.860	1.6 ( 0.4)	3.2 ( 0.3)	0.7 ( 0.1)				
15.628	1.9 ( 0.4)	2.3 ( 0.2)	0.3 ( 0.1)				
16.455	1.9 ( 0.4)	1.2 ( 0.2)					
17.437	1.6 ( 0.3)	0.4 ( 0.1)					
18.511	1.1 ( 0.2)						
19.582	0.5 ( 0.2)						
20.529	0.2 ( 0.1)						
INCIDENT ENERGY	6.01- 7.01	5.02- 6.01	4.50- 5.02	4.01- 4.50	3.50- 4.01	2.99- 3.50	2.75- 2.99
SECONDARY ENERGY (MEV)	CROSS SECTION (MB/SR/MEV)						
0.909	47.1 ( 2.4)	57.4 ( 2.7)	56.7 ( 2.9)	59.1 ( 2.6)	67.7 ( 3.1)	57.9 ( 2.7)	41.9 ( 2.3)
1.013	45.1 ( 2.3)	56.9 ( 2.4)	57.2 ( 2.6)	58.0 ( 2.3)	66.9 ( 2.8)	56.1 ( 2.3)	43.1 ( 2.1)
1.114	48.4 ( 2.1)	54.8 ( 2.2)	55.8 ( 2.5)	57.6 ( 2.2)	62.1 ( 2.5)	54.3 ( 1.9)	49.8 ( 2.2)
1.212	46.7 ( 1.9)	52.7 ( 1.9)	53.9 ( 2.3)	59.3 ( 2.1)	57.3 ( 2.2)	51.1 ( 1.6)	59.5 ( 2.3)
1.310	45.1 ( 1.8)	51.2 ( 1.8)	51.3 ( 2.1)	60.1 ( 1.9)	53.4 ( 1.9)	47.3 ( 1.4)	65.7 ( 2.2)
1.413	43.8 ( 1.6)	49.7 ( 1.6)	48.2 ( 1.9)	57.9 ( 1.7)	49.8 ( 1.7)	46.5 ( 1.3)	64.0 ( 2.0)
1.511	43.1 ( 1.5)	47.4 ( 1.5)	45.5 ( 1.7)	53.7 ( 1.6)	45.6 ( 1.6)	48.6 ( 1.3)	57.1 ( 1.9)
1.611	42.3 ( 1.4)	44.1 ( 1.4)	43.7 ( 1.6)	48.9 ( 1.4)	41.0 ( 1.4)	51.0 ( 1.3)	49.8 ( 1.8)
1.709	41.1 ( 1.3)	40.7 ( 1.3)	42.2 ( 1.5)	44.8 ( 1.4)	37.4 ( 1.2)	51.6 ( 1.2)	44.4 ( 1.6)
1.807	39.2 ( 1.3)	37.9 ( 1.3)	40.7 ( 1.6)	41.1 ( 1.5)	35.6 ( 1.3)	49.6 ( 1.2)	39.8 ( 1.5)
1.938	35.5 ( 1.2)	35.1 ( 1.1)	38.3 ( 1.5)	36.4 ( 1.5)	35.2 ( 1.3)	43.2 ( 1.2)	33.4 ( 1.5)
2.112	31.0 ( 1.0)	32.9 ( 1.0)	34.7 ( 1.1)	30.9 ( 1.0)	35.7 ( 1.0)	33.4 ( 1.0)	26.6 ( 1.3)
2.310	27.1 ( 1.0)	29.5 ( 1.0)	29.3 ( 1.2)	27.9 ( 1.2)	34.0 ( 1.2)	26.5 ( 1.0)	41.8 ( 1.3)
2.499	25.2 ( 0.8)	25.3 ( 0.8)	24.0 ( 0.9)	26.5 ( 0.9)	29.0 ( 1.0)	29.7 ( 0.9)	81.0 ( 1.5)
2.691	24.1 ( 0.7)	22.1 ( 0.7)	21.2 ( 0.8)	25.7 ( 0.9)	22.8 ( 0.8)	46.5 ( 1.1)	97.4 ( 1.6)
2.818	21.6 ( 0.7)	19.6 ( 0.7)	21.0 ( 0.8)	22.9 ( 0.8)	20.4 ( 0.8)	61.6 ( 1.1)	70.6 ( 1.3)
3.102	18.4 ( 0.6)	17.9 ( 0.7)	20.0 ( 0.9)	19.4 ( 0.9)	29.7 ( 0.9)	60.6 ( 1.2)	34.8 ( 0.8)
3.301	16.0 ( 0.6)	15.5 ( 0.7)	17.4 ( 0.8)	16.5 ( 0.9)	41.9 ( 1.1)	42.7 ( 0.9)	14.0 ( 0.4)
3.505	14.3 ( 0.7)	13.3 ( 0.6)	14.4 ( 0.7)	21.1 ( 0.8)	44.5 ( 1.0)	23.2 ( 0.5)	5.0 ( 0.2)
3.712	12.5 ( 0.7)	12.0 ( 0.6)	13.0 ( 0.6)	28.8 ( 0.8)	35.6 ( 0.8)	10.5 ( 0.3)	
3.901	10.7 ( 0.5)	11.5 ( 0.6)	14.5 ( 0.6)	31.7 ( 0.7)	23.8 ( 0.5)	4.8 ( 0.2)	
4.147	8.7 ( 0.5)	11.1 ( 0.5)	18.7 ( 0.7)	26.0 ( 0.6)	11.2 ( 0.3)	1.9 ( 0.1)	
4.457	7.9 ( 0.4)	10.8 ( 0.4)	19.5 ( 0.6)	13.1 ( 0.8)	3.7 ( 0.1)		
4.758	7.6 ( 0.4)	10.8 ( 0.4)	13.6 ( 0.4)	5.2 ( 0.2)	1.4 ( 0.1)		
5.057	7.1 ( 0.4)	10.0 ( 0.4)	6.9 ( 0.3)	1.9 ( 0.1)			
5.360	6.8 ( 0.4)	8.0 ( 0.4)	3.0 ( 0.2)	0.8 ( 0.1)			
5.644	6.5 ( 0.4)	5.5 ( 0.3)	1.8 ( 0.1)				
5.936	6.0 ( 0.3)	3.2 ( 0.2)	0.7 ( 0.1)				
6.251	4.8 ( 0.3)	1.7 ( 0.1)					
6.551	3.8 ( 0.2)	1.0 ( 0.1)					
6.833	2.2 ( 0.2)	0.7 ( 0.1)					
7.227	1.1 ( 0.1)						
7.726	0.6 ( 0.1)						
8.252	0.3 ( 0.1)						
INCIDENT ENERGY	2.51- 2.75	2.25- 2.51	2.00- 2.25	1.76- 2.00	1.49- 1.76	1.25- 1.49	1.00- 1.25
SECONDARY ENERGY (MEV)	CROSS SECTION (MB/SR/MEV)						
0.909	61.0 ( 2.5)	79.3 ( 2.8)	59.1 ( 2.4)	73.4 ( 2.5)	39.4 ( 1.5)	16.1 ( 1.3)	325.6 ( 8.5)
1.013	73.0 ( 2.6)	69.2 ( 2.5)	63.9 ( 2.4)	62.1 ( 2.0)	25.3 ( 1.2)	85.8 ( 2.2)	487.6 ( 11.3)
1.114	71.3 ( 2.4)	60.1 ( 2.2)	63.4 ( 2.1)	47.8 ( 1.6)	26.1 ( 1.2)	236.3 ( 4.8)	448.9 ( 9.7)
1.212	63.3 ( 2.1)	54.9 ( 1.9)	57.1 ( 1.9)	32.3 ( 1.2)	68.5 ( 1.9)	361.2 ( 6.8)	298.9 ( 6.4)
1.310	56.8 ( 1.9)	52.5 ( 1.7)	45.4 ( 1.5)	25.8 ( 1.1)	158.0 ( 3.4)	371.3 ( 6.7)	156.8 ( 3.3)
1.413	53.6 ( 1.8)	50.8 ( 1.6)	31.5 ( 1.2)	50.7 ( 1.3)	250.2 ( 4.9)	278.4 ( 4.9)	66.1 ( 1.4)
1.511	51.0 ( 1.7)	46.2 ( 1.5)	26.8 ( 1.1)	113.0 ( 2.2)	277.6 ( 5.1)	168.7 ( 2.9)	25.6 ( 0.6)
1.611	46.0 ( 1.6)	37.6 ( 1.3)	43.6 ( 1.2)	187.0 ( 3.1)	237.9 ( 4.2)	85.4 ( 1.5)	8.7 ( 0.1)
1.709	38.0 ( 1.4)	30.1 ( 1.1)	86.8 ( 1.7)	226.6 ( 3.6)	167.6 ( 2.9)	38.9 ( 0.7)	3.1 ( 0.1)
1.807	29.6 ( 1.2)	30.8 ( 1.1)	141.0 ( 2.4)	215.8 ( 3.3)	101.1 ( 1.7)	16.5 ( 0.3)	
1.938	24.6 ( 1.2)	72.4 ( 1.5)	182.8 ( 2.9)	151.0 ( 2.3)	43.0 ( 0.7)	4.9 ( 0.1)	
2.112	52.0 ( 1.0)	136.2 ( 2.2)	149.2 ( 2.4)	64.3 ( 1.0)	11.3 ( 0.2)		
2.310	108.6 ( 2.1)	133.6 ( 2.1)	69.6 ( 1.1)	17.3 ( 0.3)	2.4 ( 0.1)		
2.499	114.0 ( 2.2)	77.4 ( 1.2)	28.1 ( 0.4)	4.2 ( 0.1)			
2.693	72.8 ( 1.4)	31.4 ( 0.5)	7.1 ( 0.2)	1.4 ( 0.1)			
2.898	31.2 ( 0.7)	9.9 ( 0.2)	2.1 ( 0.1)				
3.102	10.7 ( 0.3)						

TABLE 2.  $CU(N, X)$  DIFFERENTIAL CROSS SECTIONS AT 130 DEGREES. THE NUMBERS IN PARENTHESIS ARE STATISTICAL UNCERTAINTIES (IN THE SAME UNITS AS THE DATA). THE OVERALL UNCERTAINTY IN NORMALIZATION IS ABOUT 10%.

TABLE 2.  $\text{Cu}(n,\gamma)$  DIFFERENTIAL CROSS SECTIONS AT 130 DEGREES. THE NUMBERS IN PARENTHESIS ARE STATISTICAL UNCERTAINTIES (IN THE SAME UNITS AS THE DATA). THE OVERALL UNCERTAINTY IN NORMALIZATION IS ABOUT 10%.

TABLE 2. CU(N,XF) DIFFERENTIAL CROSS SECTIONS AT 130 DEGREES. THE NUMBERS IN PARENTHESIS ARE STATISTICAL UNCERTAINTIES (IN THE SAME UNITS AS THE DATA). THE OVERALL UNCERTAINTY IN NORMALIZATION IS ABOUT 10%.

INCIDENT ENERGY=	17.42-20.09	14.98-17.42	12.49-14.98	9.96-12.49	9.01- 9.96	7.98- 9.01	7.02- 7.98
GAMMA RAY ENERGY (MEV)	CROSS SECTION (MB/SR/MEV)						
0.760	140.0 (26.0)	127.0 (20.7)	103.4 (19.6)	130.5 (22.2)	121.3 (25.4)	146.0 (25.2)	142.2 (24.2)
0.800	149.2 ( 9.2)	125.2 ( 7.2)	117.9 ( 6.6)	150.7 ( 7.0)	151.7 ( 8.5)	161.3 ( 8.2)	157.2 ( 7.9)
0.840	156.0 ( 5.3)	135.6 ( 4.0)	138.8 ( 3.4)	179.6 ( 3.3)	188.0 ( 4.4)	199.8 ( 4.1)	191.9 ( 3.9)
0.880	178.1 ( 4.8)	157.3 ( 3.6)	166.4 ( 3.1)	217.5 ( 3.0)	236.1 ( 4.0)	252.5 ( 3.7)	243.5 ( 3.5)
0.920	206.8 ( 5.0)	179.3 ( 3.8)	192.1 ( 3.2)	250.3 ( 3.1)	275.4 ( 4.2)	294.4 ( 3.9)	287.4 ( 3.7)
0.960	227.0 ( 4.9)	190.4 ( 3.7)	207.0 ( 3.2)	264.9 ( 3.1)	288.3 ( 4.1)	305.0 ( 3.9)	301.8 ( 3.7)
1.000	236.7 ( 4.9)	194.1 ( 3.7)	212.3 ( 3.1)	264.6 ( 3.0)	278.5 ( 4.0)	289.5 ( 3.7)	289.1 ( 3.5)
1.040	246.3 ( 4.8)	202.2 ( 3.6)	216.3 ( 3.0)	260.9 ( 2.8)	259.1 ( 3.8)	265.4 ( 3.5)	266.1 ( 3.3)
1.080	258.9 ( 4.8)	217.1 ( 3.6)	222.7 ( 3.0)	257.5 ( 2.8)	239.5 ( 3.7)	243.2 ( 3.4)	244.5 ( 3.2)
1.125	265.6 ( 4.7)	228.9 ( 3.5)	227.3 ( 3.0)	249.4 ( 2.8)	221.4 ( 3.6)	221.7 ( 3.3)	224.2 ( 3.1)
1.175	255.4 ( 4.5)	222.3 ( 3.4)	221.0 ( 2.9)	234.3 ( 2.7)	208.3 ( 3.5)	205.2 ( 3.2)	207.7 ( 3.1)
1.225	231.8 ( 4.4)	199.9 ( 3.4)	205.4 ( 3.0)	221.4 ( 2.8)	205.6 ( 3.8)	204.2 ( 3.5)	203.0 ( 3.3)
1.275	203.3 ( 4.4)	173.9 ( 3.3)	188.0 ( 3.0)	215.5 ( 2.9)	210.0 ( 3.9)	213.9 ( 3.6)	208.6 ( 3.4)
1.325	175.4 ( 3.8)	150.3 ( 2.9)	170.4 ( 2.5)	210.4 ( 2.5)	210.8 ( 3.4)	218.5 ( 3.2)	213.2 ( 3.0)
1.375	151.0 ( 3.5)	130.2 ( 2.6)	150.5 ( 2.3)	199.5 ( 2.2)	201.6 ( 3.0)	209.1 ( 2.8)	207.4 ( 2.7)
1.425	131.8 ( 3.5)	114.0 ( 2.6)	129.5 ( 2.3)	182.0 ( 2.3)	185.1 ( 3.2)	190.3 ( 2.9)	191.1 ( 2.8)
1.475	117.2 ( 3.5)	101.5 ( 2.5)	110.6 ( 2.1)	160.9 ( 2.1)	166.6 ( 3.0)	170.0 ( 2.7)	170.0 ( 2.6)
1.525	106.8 ( 3.3)	91.9 ( 2.4)	95.3 ( 2.0)	139.5 ( 2.0)	108.1 ( 2.8)	151.4 ( 2.5)	148.6 ( 2.4)
1.575	99.2 ( 3.1)	83.4 ( 2.2)	83.0 ( 1.9)	120.0 ( 1.9)	129.7 ( 2.6)	133.6 ( 2.4)	128.8 ( 2.3)
1.640	91.8 ( 3.0)	72.4 ( 2.2)	71.3 ( 1.9)	100.8 ( 1.8)	108.8 ( 2.6)	113.3 ( 2.3)	108.2 ( 2.2)
1.720	83.9 ( 2.9)	61.0 ( 2.1)	61.7 ( 1.8)	89.4 ( 1.7)	93.8 ( 2.4)	99.4 ( 2.2)	94. ( 2.1)
1.800	77.2 ( 2.9)	56.4 ( 2.0)	56.7 ( 1.7)	84.5 ( 1.7)	89.2 ( 2.4)	95.3 ( 2.2)	90.4 ( 2.0)
1.880	71.8 ( 2.7)	55.0 ( 2.0)	55.6 ( 1.7)	78.0 ( 1.7)	85.5 ( 2.3)	90.0 ( 2.1)	87.0 ( 2.0)
1.960	65.6 ( 2.8)	50.6 ( 2.0)	53.0 ( 1.7)	70.8 ( 1.7)	77.7 ( 2.4)	81.2 ( 2.2)	80.1 ( 2.0)
2.040	58.4 ( 2.6)	43.1 ( 1.8)	45.6 ( 1.6)	65.4 ( 1.6)	67.9 ( 2.2)	73.7 ( 2.0)	72.3 ( 1.9)
2.120	51.9 ( 2.5)	36.6 ( 1.8)	36.8 ( 1.6)	59.5 ( 1.5)	59.6 ( 2.2)	68.0 ( 2.0)	66.0 ( 1.8)
2.200	47.1 ( 2.4)	33.3 ( 1.7)	31.2 ( 1.5)	51.6 ( 1.5)	55.0 ( 2.1)	62.2 ( 1.9)	60.8 ( 1.8)
2.280	43.9 ( 2.3)	31.3 ( 1.6)	29.0 ( 1.5)	44.3 ( 1.4)	53.2 ( 2.0)	56.7 ( 1.8)	55.1 ( 1.7)
2.360	41.3 ( 2.3)	28.1 ( 1.6)	27.5 ( 1.5)	40.8 ( 1.4)	51.5 ( 2.0)	52.8 ( 1.8)	49.3 ( 1.7)
2.450	37.2 ( 2.2)	23.6 ( 1.5)	25.7 ( 1.4)	40.8 ( 1.4)	48.7 ( 2.0)	49.9 ( 1.8)	45.3 ( 1.6)
2.550	31.2 ( 2.0)	20.7 ( 1.4)	24.5 ( 1.3)	41.7 ( 1.3)	46.5 ( 1.9)	46.9 ( 1.7)	44.6 ( 1.5)
2.650	26.5 ( 2.0)	20.4 ( 1.4)	23.9 ( 1.4)	40.9 ( 1.3)	46.0 ( 1.9)	44.1 ( 1.7)	44.0 ( 1.5)
2.750	25.3 ( 1.9)	20.3 ( 1.4)	22.8 ( 1.3)	38.9 ( 1.3)	44.7 ( 1.8)	42.4 ( 1.6)	41.2 ( 1.5)
2.850	26.3 ( 1.9)	19.0 ( 1.3)	21.7 ( 1.3)	36.9 ( 1.3)	42.2 ( 1.9)	41.5 ( 1.6)	38.0 ( 1.4)
2.950	26.5 ( 1.9)	16.8 ( 1.3)	20.5 ( 1.3)	35.0 ( 1.3)	39.9 ( 1.8)	40.1 ( 1.6)	36.5 ( 1.4)
3.050	25.5 ( 1.9)	14.9 ( 1.3)	19.0 ( 1.3)	33.1 ( 1.3)	38.1 ( 1.8)	38.4 ( 1.6)	36.5 ( 1.4)
3.150	23.5 ( 1.9)	13.3 ( 1.3)	17.7 ( 1.3)	31.4 ( 1.3)	36.0 ( 1.8)	36.9 ( 1.6)	36.2 ( 1.4)
3.250	20.8 ( 1.9)	11.5 ( 1.3)	17.0 ( 1.3)	30.1 ( 1.3)	33.6 ( 1.8)	35.6 ( 1.6)	34.7 ( 1.4)
3.350	18.0 ( 1.8)	9.6 ( 1.3)	17.1 ( 1.3)	29.2 ( 1.3)	31.8 ( 1.8)	34.2 ( 1.6)	32.3 ( 1.4)
3.450	16.2 ( 1.8)	8.6 ( 1.3)	17.5 ( 1.3)	28.7 ( 1.3)	30.8 ( 1.8)	32.1 ( 1.5)	29.9 ( 1.3)
3.550	15.6 ( 1.7)	9.1 ( 1.3)	17.4 ( 1.3)	28.5 ( 1.3)	30.0 ( 1.9)	30.0 ( 1.5)	28.1 ( 1.3)
3.665	15.7 ( 1.7)	10.6 ( 1.3)	15.9 ( 1.4)	27.8 ( 1.4)	28.4 ( 1.8)	28.3 ( 1.5)	26.3 ( 1.3)
3.795	15.3 ( 1.8)	11.7 ( 1.3)	13.4 ( 1.4)	26.0 ( 1.3)	26.7 ( 1.8)	27.5 ( 1.5)	23.9 ( 1.3)
3.925	14.0 ( 1.8)	11.3 ( 1.3)	11.9 ( 1.4)	24.3 ( 1.4)	26.5 ( 1.8)	26.6 ( 1.5)	22.0 ( 1.3)
4.055	12.3 ( 1.8)	9.6 ( 1.4)	11.8 ( 1.5)	23.7 ( 1.4)	27.2 ( 1.9)	24.9 ( 1.6)	21.4 ( 1.3)
4.185	11.0 ( 1.8)	7.1 ( 1.5)	12.3 ( 1.5)	23.7 ( 1.5)	26.6 ( 2.0)	23.5 ( 1.6)	20.9 ( 1.3)
4.315	10.1 ( 1.9)	4.7 ( 1.5)	13.0 ( 1.6)	22.9 ( 1.6)	24.4 ( 2.1)	22.5 ( 1.7)	19.4 ( 1.4)
4.445	9.1 ( 2.0)	3.0 ( 1.6)	13.7 ( 1.8)	20.8 ( 1.7)	21.0 ( 2.2)	21.1 ( 1.8)	17.2 ( 1.4)
4.575	7.6 ( 1.9)	2.8 ( 1.7)	13.9 ( 1.9)	19.3 ( 1.8)	17.8 ( 2.4)	19.0 ( 1.9)	15.3 ( 1.5)
4.705	6.1 ( 1.9)	3.9 ( 1.7)	12.9 ( 1.9)	16.2 ( 1.9)	15. ( 2.4)	17.0 ( 1.8)	14.1 ( 1.4)
4.835	5.3 ( 1.9)	5.9 ( 1.8)	10.5 ( 2.0)	14.9 ( 2.0)	14.8 ( 2.4)	15.7 ( 1.9)	13.0 ( 1.4)
4.985	5.4 ( 1.9)	8.2 ( 1.8)	7.1 ( 2.1)	14.3 ( 2.1)	15.6 ( 2.6)	14.9 ( 2.0)	11.5 ( 1.5)
5.155	6.2 ( 2.0)	9.0 ( 1.8)	5.1 ( 2.3)	14.6 ( 2.3)	17.4 ( 2.7)	13.8 ( 2.0)	9.6 ( 1.5)
5.325	6.8 ( 1.9)	7.4 ( 1.8)	6.1 ( 2.3)	15.5 ( 2.3)	17.9 ( 2.8)	11.5 ( 2.0)	8.3 ( 1.5)
5.495	6.5 ( 1.9)	4.3 ( 1.9)	8.9 ( 2.3)	15.4 ( 2.4)	15.8 ( 2.8)	8.9 ( 2.0)	7.7 ( 1.4)
5.665	5.0 ( 1.8)	1.7 ( 1.8)	11.0 ( 2.3)	13.8 ( 2.4)	12.0 ( 2.8)	7.5 ( 1.9)	7.1 ( 1.3)
5.835	3.2 ( 1.7)	0.8 ( 1.7)	10.9 ( 2.2)	11.1 ( 2.3)	8. ( 2.6)	7.3 ( 1.7)	6.1 ( 1.2)
6.005	2.1 ( 1.5)	1.6 ( 1.5)	8.6 ( 2.0)	8.7 ( 2.1)	6.2 ( 2.3)	7.4 ( 1.6)	4.7 ( 1.0)
6.175	1.8 ( 1.3)	2.8 ( 1.4)	5.6 ( 1.9)	7.7 ( 2.0)	5.8 ( 2.2)	6.9 ( 1.4)	3.5 ( 0.9)
6.345	1.9 ( 1.2)	3.5 ( 1.3)	3.4 ( 1.7)	7.7 ( 1.8)	6.2 ( 1.9)	6.1 ( 1.1)	2.8 ( 0.7)
6.515	2.0 ( 1.0)	3.3 ( 1.1)	2.6 ( 1.4)	8.1 ( 1.5)	6.7 ( 1.5)	5.1 ( 1.0)	2.3 ( 0.6)
6.700	1.8 ( 0.8)	2.4 ( 0.9)	3.0 ( 1.1)	7.9 ( 1.2)	6.8 ( 1.2)	4.5 ( 0.7)	1.9 ( 0.4)
6.900	1.2 ( 0.7)	1.5 ( 0.7)	3.5 ( 0.9)	6.8 ( 1.0)	5.8 ( 1.0)	3.8 ( 0.5)	1.5 ( 0.3)
7.100	0.7 ( 0.6)	1.2 ( 0.6)	3.4 ( 0.8)	5.2 ( 0.9)	4.2 ( 0.8)	3.0 ( 0.4)	1.0 ( 0.2)
7.300	0.4 ( 0.5)	1.4 ( 0.5)	2.8 ( 0.7)	3.8 ( 0.8)	2.6 ( 0.7)	2.2 ( 0.3)	0.7 ( 0.2)
7.500	0.5 ( 0.4)	1.5 ( 0.5)	2.1 ( 0.6)	3.0 ( 0.7)	1.5 ( 0.6)	1.4 ( 0.2)	0.4 ( 0.1)
7.700	0.6 ( 0.3)	1.5 ( 0.3)	1.5 ( 0.5)	2.5 ( 0.5)	1.0 ( 0.5)	0.9 ( 0.1)	0.3 ( 0.1)
7.900	0.7 ( 0.2)	1.2 ( 0.3)	1.1 ( 0.4)	2.0 ( 0.4)	0.9 ( 0.4)	0.5 ( 0.1)	0.2 ( 0.1)
8.100	0.6 ( 0.2)	0.8 ( 0.2)	0.8 ( 0.3)	1.6 ( 0.4)	1.0 ( 0.3)	0.3 ( 0.1)	0.1 ( 0.1)
8.300	0.5 ( 0.2)	0.4 ( 0.2)	0.7 ( 0.3)	1.2 ( 0.3)	0.9 ( 0.3)	0.2 ( 0.1)	0.1 ( 0.1)
8.500	0.3 ( 0.1)	0.1 ( 0.2)	0.6 ( 0.2)	0.9 ( 0.3)	0.7 ( 0.2)	0.1 ( 0.1)	0.0 ( 0.1)
8.725	0.2 ( 0.1)	-0.0 ( 0.1)	0.5 ( 0.2)	0.6 ( 0.2)	0.5 ( 0.2)	0.0 ( 0.1)	0.0 ( 0.1)
8.975	0.1 ( 0.1)	-0.1 ( 0.1)	0.4 ( 0.2)	0.4 ( 0.2)	0.2 ( 0.1)	0.0 ( 0.1)	0.0 ( 0.1)
9.225	0.0 ( 0.1)	-0.1 ( 0.1)	0.2 ( 0.1)	0.2 ( 0.1)	0.0 ( 0.1)	0.0 ( 0.1)	0.0 ( 0.1)
9.475	0.0 ( 0.1)	-0.0 ( 0.1)	0.1 ( 0.1)	0.1 ( 0.1)	-0.0 ( 0.1)	0.0 ( 0.1)	0.0 ( 0.1)
9.725	0.0 ( 0.1)	-0.0 ( 0.1)	0.0 ( 0.1)	0.0 ( 0.1)	-0.1 ( 0.1)	0.0 ( 0.1)	0.0 ( 0.1)
9.975	0.0 ( 0.1)	0.0 ( 0.1)	-0.0 ( 0.1)	0.0 ( 0.1)	-0.1 ( 0.1)	0.0 ( 0.1)	0.0 ( 0.1)

TABLE 3. TOTAL SECONDARY YIELDS AND AVERAGE SECONDARY ENERGIES FOR NEUTRONS AND GAMMA RAYS DUE TO NEUTRON INTERACTIONS WITH COPPER. THESE RESULTS ARE FOR SECONDARY NEUTRONS WITH ENERGIES GREATER THAN 0.756 MEV AND GAMMA RAYS WITH ENERGIES GREATER THAN 0.700 MEV. UNCERTAINTIES ARE GIVEN IN PARENTHESES IN THE SAME UNITS AS THE DATA. UNCERTAINTIES IN TOTAL YIELDS DO NOT INCLUDE A 10% ERROR IN ABSOLUTE NORMALIZATION. THE ANGLE IS 130 DEGREES.

INCIDENT NEUTRON ENERGY (MEV)	ENERGY SPREAD	SECONDARY NEUTRON YIELD (MB/SR)	AVERAGE NEUTRON ENERGY (MEV)	SECONDARY PHOTON YIELD (MB/SR)	AVERAGE PHOTON ENERGY (MEV)
1.026	0.048	190.58 (1.80)	1.011 (.013)	12.33 (.30)	1.284 (.043)
1.076	0.052	192.98 (1.71)	1.044 (.012)	14.66 (0.30)	1.181 (.034)
1.124	0.044	194.73 (1.94)	1.020 (.013)	16.20 (0.35)	1.177 (.035)
1.175	0.059	200.56 (1.79)	1.042 (.010)	22.00 (0.35)	1.127 (.024)
1.230	0.050	183.04 (1.88)	1.159 (.012)	23.97 (0.38)	1.107 (.024)
1.275	0.040	168.31 (2.05)	1.275 (.016)	27.03 (0.46)	1.092 (.025)
1.323	0.056	157.56 (1.89)	1.333 (.015)	27.98 (0.40)	1.115 (.021)
1.373	0.045	167.29 (2.14)	1.313 (.015)	32.40 (0.48)	1.113 (.022)
1.419	0.047	165.42 (1.98)	1.288 (.014)	35.58 (0.48)	1.103 (.020)
1.467	0.049	170.73 (1.86)	1.286 (.012)	40.49 (0.49)	1.106 (.018)
1.518	0.052	167.60 (1.71)	1.326 (.012)	44.16 (0.49)	1.128 (.016)
1.571	0.055	153.43 (1.53)	1.402 (.013)	47.39 (0.50)	1.139 (.015)
1.627	0.058	151.50 (1.44)	1.475 (.013)	52.71 (0.51)	1.154 (.014)
1.676	0.040	139.72 (1.58)	1.550 (.017)	55.05 (0.62)	1.164 (.017)
1.728	0.063	147.04 (1.45)	1.557 (.014)	59.29 (0.53)	1.177 (.013)
1.781	0.044	151.68 (1.69)	1.564 (.016)	65.02 (0.68)	1.176 (.016)
1.826	0.046	154.36 (1.69)	1.567 (.015)	63.33 (0.65)	1.189 (.015)
1.872	0.047	159.19 (1.74)	1.550 (.015)	68.98 (0.67)	1.176 (.015)
1.921	0.049	160.77 (1.69)	1.581 (.015)	72.76 (0.69)	1.183 (.014)
1.971	0.051	155.72 (1.58)	1.633 (.015)	74.06 (0.69)	1.204 (.014)
2.051	0.109	149.43 (1.17)	1.699 (.012)	78.52 (0.51)	1.218 (.010)
2.149	0.087	146.71 (1.15)	1.734 (.014)	84.02 (0.61)	1.220 (.011)
2.239	0.093	148.79 (1.14)	1.754 (.014)	91.21 (0.65)	1.222 (.011)
2.344	0.116	153.70 (1.07)	1.780 (.013)	99.76 (0.64)	1.236 (.010)
2.455	0.107	149.78 (1.09)	1.832 (.015)	108.19 (0.73)	1.230 (.010)
2.556	0.095	144.31 (1.17)	1.900 (.018)	115.49 (0.87)	1.241 (.012)
2.653	0.100	138.58 (1.20)	1.970 (.020)	124.13 (0.96)	1.262 (.012)
2.756	0.106	133.87 (1.39)	2.010 (.023)	128.46 (1.11)	1.273 (.014)
2.854	0.089	136.50 (1.54)	2.046 (.025)	134.87 (1.24)	1.275 (.015)
2.945	0.094	140.20 (1.54)	2.038 (.024)	143.11 (1.24)	1.297 (.014)
3.041	0.098	141.07 (1.50)	2.029 (.023)	153.10 (1.22)	1.306 (.013)
3.142	0.103	136.88 (1.46)	2.091 (.024)	158.85 (1.21)	1.321 (.013)
3.247	0.108	132.38 (1.44)	2.147 (.025)	165.30 (1.21)	1.337 (.012)
3.344	0.085	133.57 (1.52)	2.162 (.028)	171.41 (1.39)	1.351 (.014)
3.446	0.118	137.00 (1.29)	2.117 (.023)	181.30 (1.21)	1.361 (.011)
3.551	0.093	137.61 (1.42)	2.145 (.027)	190.64 (1.41)	1.379 (.013)
3.646	0.097	134.48 (1.36)	2.170 (.028)	196.95 (1.40)	1.392 (.012)
3.745	0.101	133.98 (1.31)	2.172 (.028)	203.90 (1.40)	1.402 (.012)
3.848	0.105	137.67 (1.31)	2.197 (.027)	210.94 (1.39)	1.429 (.012)
3.955	0.109	132.08 (1.28)	2.214 (.027)	220.71 (1.40)	1.439 (.011)
4.047	0.075	133.09 (1.55)	2.233 (.032)	224.26 (1.71)	1.447 (.014)
4.144	0.117	132.88 (1.27)	2.254 (.027)	231.04 (1.39)	1.464 (.011)
4.243	0.081	130.24 (1.53)	2.261 (.032)	237.58 (1.72)	1.478 (.013)
4.346	0.126	131.54 (1.24)	2.241 (.027)	242.27 (1.43)	1.493 (.011)
4.453	0.087	131.27 (1.46)	2.238 (.032)	246.44 (1.74)	1.515 (.013)
4.541	0.090	125.72 (1.43)	2.295 (.033)	253.24 (1.75)	1.531 (.013)
4.632	0.092	127.89 (1.45)	2.278 (.032)	264.01 (1.77)	1.547 (.013)
4.750	0.144	123.23 (1.25)	2.321 (.028)	264.54 (1.42)	1.567 (.011)
4.872	0.100	121.23 (1.44)	2.386 (.033)	273.88 (1.75)	1.574 (.013)
4.974	0.103	126.12 (1.44)	2.335 (.032)	284.78 (1.77)	1.600 (.013)
5.105	0.160	120.19 (1.19)	2.373 (.028)	285.27 (1.45)	1.616 (.010)
5.299	0.226	123.11 (1.06)	2.320 (.024)	292.19 (1.25)	1.646 (.009)
5.501	0.180	122.28 (1.15)	2.340 (.026)	298.71 (1.44)	1.674 (.010)
5.702	0.221	120.35 (1.07)	2.359 (.025)	302.67 (1.32)	1.702 (.009)
5.912	0.200	120.06 (1.12)	2.387 (.026)	306.57 (1.41)	1.719 (.010)
6.100	0.175	117.24 (1.18)	2.435 (.029)	307.41 (1.53)	1.755 (.011)
6.297	0.220	115.78 (1.08)	2.470 (.027)	311.71 (1.38)	1.770 (.010)
6.503	0.192	114.64 (1.15)	2.523 (.030)	316.92 (1.50)	1.788 (.011)
6.700	0.201	114.34 (1.13)	2.540 (.030)	319.64 (1.49)	1.820 (.011)
6.906	0.211	115.26 (1.11)	2.602 (.030)	324.29 (1.49)	1.842 (.011)
7.099	0.176	111.04 (1.19)	2.689 (.035)	329.66 (1.66)	1.859 (.012)
7.302	0.229	112.72 (1.09)	2.670 (.032)	328.19 (1.48)	1.911 (.011)
7.512	0.191	108.63 (1.16)	2.793 (.037)	327.19 (1.63)	1.917 (.012)
7.707	0.199	109.94 (1.11)	2.783 (.037)	325.93 (1.61)	1.948 (.013)
7.910	0.207	104.65 (1.03)	2.904 (.039)	316.35 (1.55)	1.966 (.013)
8.094	0.161	107.59 (1.17)	2.930 (.045)	325.06 (1.80)	1.970 (.014)
8.285	0.222	108.43 (1.03)	2.996 (.042)	340.47 (1.61)	2.023 (.013)
8.511	0.231	115.06 (1.05)	3.035 (.043)	347.40 (1.64)	2.042 (.013)
8.716	0.179	112.83 (1.19)	3.094 (.048)	351.47 (1.90)	2.063 (.015)
8.899	0.185	110.82 (1.16)	3.100 (.047)	344.97 (1.85)	2.074 (.015)
9.087	0.191	104.85 (1.10)	3.137 (.048)	335.32 (1.78)	2.075 (.015)
9.281	0.197	102.15 (1.07)	3.164 (.048)	329.31 (1.74)	2.095 (.015)
9.481	0.204	103.43 (1.10)	3.287 (.050)	338.61 (1.79)	2.109 (.015)
9.689	0.211	106.85 (1.13)	3.337 (.051)	351.93 (1.85)	2.137 (.015)
9.903	0.218	110.05 (1.15)	3.459 (.053)	355.30 (1.87)	2.139 (.015)
10.240	0.458	111.48 (0.85)	3.563 (.042)	359.44 (1.34)	2.160 (.011)
10.714	0.490	110.04 (0.85)	3.693 (.045)	348.80 (1.30)	2.165 (.011)
11.222	0.525	107.02 (0.88)	3.853 (.050)	334.37 (1.28)	2.159 (.011)
11.718	0.467	112.72 (0.96)	3.932 (.056)	325.58 (1.44)	2.146 (.013)
12.252	0.600	110.96 (0.86)	3.913 (.054)	294.11 (1.26)	2.101 (.012)
12.764	0.425	120.36 (1.16)	3.804 (.064)	275.48 (1.58)	2.072 (.016)
13.258	0.563	125.67 (1.11)	3.707 (.058)	249.92 (1.36)	2.028 (.015)
13.779	0.478	135.24 (1.39)	3.796 (.066)	237.95 (1.55)	1.963 (.017)
14.269	0.503	138.13 (1.44)	3.671 (.065)	221.25 (1.51)	1.908 (.018)
14.787	0.531	134.47 (1.46)	3.662 (.069)	213.96 (1.50)	1.844 (.018)
15.261	0.418	141.94 (1.77)	3.825 (.083)	213.98 (1.82)	1.810 (.021)
15.763	0.585	146.96 (1.65)	3.718 (.074)	209.48 (1.58)	1.770 (.018)
16.286	0.461	146.66 (1.89)	3.649 (.086)	208.33 (1.84)	1.727 (.020)
16.758	0.482	151.24 (1.96)	3.750 (.089)	219.73 (1.93)	1.728 (.020)
17.250	0.503	159.48 (2.07)	3.566 (.088)	230.58 (2.04)	1.728 (.020)
17.764	0.526	166.68 (2.18)	3.693 (.092)	247.75 (2.20)	1.726 (.020)
18.303	0.550	164.36 (2.19)	3.690 (.096)	255.27 (2.26)	1.750 (.020)
18.768	0.381	169.96 (2.70)	3.741 (.118)	274.70 (2.92)	1.731 (.024)
19.256	0.594	171.48 (2.31)	3.681 (.102)	280.32 (2.45)	1.790 (.021)
19.759	0.412	174.62 (2.81)	3.769 (.126)	291.41 (3.12)	1.815 (.026)



ORNL-5499  
ENDF-273  
Dist. Category UC-34c

## INTERNAL DISTRIBUTION

- |                               |                                    |
|-------------------------------|------------------------------------|
| 1. L. S. Abbott               | 26. R. W. Peelle                   |
| 2. R. G. Alsmiller, Jr.       | 27. F. G. Perey                    |
| 3. C. F. Barnett              | 28-30. RSIC                        |
| 4. D. E. Bartine              | 31. D. Steiner                     |
| 5. G. T. Chapman              | 32. M. L. Tobias                   |
| 6. G. de Saussure             | 33. C. R. Weisbin                  |
| 7. J. K. Dickens              | 34. A. Zucker                      |
| 8. G. F. Flanagan             | 35. Paul Greebler (Consultant)     |
| 9. C. Y. Fu                   | 36. W. B. Loewenstein (Consultant) |
| 10. H. Goldstein (Consultant) | 37. R. E. Uhrig (Consultant)       |
| 11. D. C. Larson              | 38. Richard Wilson (Consultant)    |
| 12. F. C. Maienschein         | 39-40. Central Research Library    |
| 13-22. G. L. Morgan           | 41. ORNL - Y-12 Technical Library  |
| 23. O. B. Morgan              | 42. Laboratory Records, ORNL RC    |
| 24. E. M. Oblow               | 43. ORNL Patent Office             |
| 25. D. K. Olsen               | 44-45. Laboratory Records          |

## EXTERNAL DISTRIBUTION

46. John D. Anderson, Physics Dept., E Division, Lawrence Livermore Laboratory, Livermore, CA 94550
47. D. Auton, Defense Nuclear Agency, Tactical Nuclear Division, Washington, DC 20305
48. H. H. Barschall, Dept. of Physics, University of Wisconsin, Madison, WI 53706
49. R. C. Block, Nuclear Eng. & Science Dept., RPI, Troy, NY 12181
50. C. D. Bowman, Nuclear Sciences Division, RAD/P, NBS, Washington, DC 20234
51. R. E. Chrien, Physics Dept., 570A, BNL, Upton, NY 11973
52. C. L. Cowan, General Electric Company - BRDO, 310 de Guigne Drive, Sunnyvale, CA 94086
53. R. A. Dannels, Westinghouse Electric Corp., Nuclear Energy Systems, P. O. Box 355, Pittsburgh, PA 15230
54. D. Dudziak, Los Alamos Scientific Laboratory, Los Alamos, NM 87545
55. D. R. Finch, E. I. Dupont de Nemours & Co., Savannah River Lab., P. O. Box 117, Aiken, SC 29801
56. E. G. Fuller, B102 Radiation Physics Building, NBS, Washington, DC 20234
57. S. Gerstl, Los Alamos Scientific Laboratory, Los Alamos, NM 87544
58. R. C. Haight, Lawrence Livermore Laboratory, Livermore, CA 94550
59. J. Hardy, Bettis Atomic Power Laboratory, P. O. Box 79, West Mifflin, PA 15122
60. P. B. Hemmig, Div. of Reactor Dev. & Demonstration, DOE, Washington, DC 20545
61. N. E. Holden, KAPL, P. O. Box 1072, Schenectady, NY 12301
62. R. J. Howerton, LLL, Livermore, CA 94550

- 63. H. H. HummeII, Bldg. 208, Room W-205, ANL, Argonne, IL 60439
- 64. H. E. Jackson, ANL, Argonne, IL 60439
- 65. M. Kalos, AEC Computing & App. Math. Center, Courant Inst. of Math Sciences, New York Univ., 251 Mercer St., New York, NY 10012
- 66. R. J. LaBauve, LASL, P.O. Box 1663, Los Alamos, NM 87545
- 67. B. Leonard, Battelle-Northwest, P.O. Box 999, Richland, WA 99352
- 68. A. E. Livolsi, Babcock & Wilcox Co., Power Generation Division, P.O. Box 1260, Lynchburg, VA 24505
- 69. C. R. Lubitz, G2-316, KAPL, P.O. Box 1072, Schenectady, NY 12301
- 70. D. Mathews, Gulf General Atomic, P.O. Box 608, San Diego, CA 92112
- 71. C. W. Maynard, University of Wisconsin, Madison, WI 53706
- 72. J. McCrosson, E. I. Dupont de Nemours & Co., Savannah River Lab., P.O. Box 117, Aiken, SC 29801
- 73. W. McElroy, HEDL, P.O. Box 1970, Richland, WA 99352
- 74. Michael S. Moore, P. Division, LASL, Los Alamos, NM 87545
- 75. D. W. Muir, LASL, Los Alamos, NM 87545
- 76. R. J. Neuhold, Division of Reactor Development and Demonstration, DOE, Washington, DC 20545
- 77. H. W. Newson, Dept. of Physics, Duke Univ., Durham, NC 27706
- 78. V. J. Orphan, Science Applications, Inc., P.O. Box 2351, La Jolla, CA 92037
- 79. N. C. Paik, Westinghouse Electric Corp., Advanced Reactor Div., Waltz Mill Site, P.O. Box 158, Madison, PA 15663
- 80. S. Pearlstein, National Nuclear Data Center, BNL, Upton, NY 11973
- 81. E. M. Pennington, Bldg. 208, ANL, Argonne, IL 60439
- 82. G. L. Rogosa, DPR, DOE, Washington, DC 20545
- 83. Robert Schenter, HEDL, P.O. Box 1970, Richland, WA 99352
- 84. R. Sher, Dept. of Mechanical Engineering, Stanford University, Stanford, CA 94305
- 85. A. B. Smith, ANL, Argonne, IL 60439
- 86. Leona Stewart, LASL, MS-243, Los Alamos, NM 87544
- 87. Bruce Twining, Systems and Applications Studies Branch, Div. of Controlled Thermonuclear Research, DOE, Washington, DC 20545
- 88. W. H. Walker, Applied Mathematics Branch, Chalk River Nuclear Laboratory, Atomic Energy of Canada, Ltd., Chalk River, Ontario, Canada
- 89. Stanley L. Whetstone, Div. of Basic Energy Sciences, DOE, Washington, DC 20545
- 90. J. M. Williams, Div. of Controlled Thermonuclear Research, DOE, Washington, DC 20545
- 91. P. G. Young, LASL, Los Alamos, NM 87545
- 92. Assistant Manager, Energy Research and Development, DOE-ORO
- 93-184. Bonnie McNair, National Nuclear Data Center, ENDF, Brookhaven National Laboratory, Upton, NY 11973
- 185-307. Given distribution as shown in TID-4500 under distribution category UC-34c